ICUS REPORT 2009 - 04

INTERNATIONAL CENTER FOR
URBAN SAFETY ENGINEERING

INSTITUTE OF INDUSTRIAL SCIENCE
THE UNIVERSITY OF TOKYO

RNUS ANNUAL REPORT 2008-2009

Edited by

Kawin Worakanchana,
Pennung Warnitchai and Kimiro Meguro

ICUS, IIS, The University of Tokyo, Japan

ISBN4-903661-32-6

Serial Number 40

RNUS Annual Report 2008 and 2009

Seismic Hazard Assessment in Thailand

Edited by

Kawin Worakanchana, Pennung Warnitchai
and Kimiro Meguro

International Center for Urban Safety Engineering (ICUS)
Institute of Industrial Science
The University of Tokyo, Japan

ICUS Report No.40
November 2009

PREFACE

This report describes seismic hazard assessment in Thailand as a part of RNUS activities in 2008 and 2009. This activity was under the research project: "Master Plan for Earthquake and Building Collapse Hazard Prevention and Mitigation in Thailand (Phase I)" which was initiated and sponsored by the Department of Disaster Prevention and Mitigation (DDPM) under Thailand's Ministry of Interior. This project was carried out by the joint consulting team of RNUS, the Asian Institute of Technology (AIT) and Panya Consultants Co. Ltd.

The objective of seismic hazard assessment is to develop the seismic hazard map which is an essential tool for developing pro-active strategy for mitigating earthquake disaster. This map can be beneficial for mitigating earthquake disaster by providing proper value of earthquake level for seismic designs of building and infrastructure. Moreover, it will be used to prepare adequate resources such as the number of officers and equipments required for earthquake disaster mitigation. It can be also used for specifying the earthquake insurance premium in each region of the country.

Kawin Worakanchana, Pennung Warnitchai
and Kimiro Meguro

CONTENTS

RNUS ANNUAL REPORT 2008 and 2009

SEISMIC HAZARD ASSESSMENT IN THAILAND

KAWIN WORAKANCHANA
International Center for Urban Safety Engineering
Institute of Industrial Science
The University of Tokyo, JAPAN

PENNUNG WARNITCHAI
School of Engineering and Technology
Asian Institute of Technology, THAILAND

KIMIRO MEGURO
International Center for Urban Safety Engineering
Institute of Industrial Science
The University of Tokyo, JAPAN

1. INTRODUCTION

This report describes the seismic hazard assessment in Thailand which is a part of the research project: "Master Plan for Earthquake and Building Collapse Hazard Prevention and Mitigation in Thailand (Phase I)". This project was initiated and funded by the Department of Disaster Prevention and Mitigation (DDPM) under the Thailand's Ministry of Interior.. The work has been carried out by the consulting team consisting of RNUS, Asian Institute of Technology (AIT) and Panya Consultants Co. Ltd.

Tsunami generated from the 2004 Sumatra earthquake has brought one of the most tragic disasters to Thai people. After the event, most Thai people began to realize how destructive an earthquake can be. They also perceive that large earthquakes tend to occur more frequently in Thailand and its neighbouring countries. Moreover, geological studies indicate that potential seismic sources can affect 61 provinces out of the total 76. DDPM has foreseen the possibility of earthquake destruction; therefore it initiated the project to provide a pro-active strategy for mitigating future earthquake disasters. This plan will be used as a supplement to the national disaster prevention and mitigation plan for a wide range of Thailand's organizations which include ministries, departments, districts and local government units, private entities, foundations, non-profit and non-government organizations to further varies develop an earthquake disaster managing system.

This report consists of five parts. The first part in this project describes the study area and development of the earthquake catalog. Then, the second part contains information about the earthquake source models. The third one discusses the results obtained from the seismic hazard studies.

The probabilistic seismic hazard (PSHA) map in this report has been carried out using the most updated earthquake catalog until 2007. It is also the first PSHA map for Thailand that includes the effect from faults. We also adopted the spatially smoothed seismicity model (Frankel, 1995) to improve the subjective judgment from delineation of areas used in the traditional approach for model background seismicity.

The map will have the important role in the earthquake mitigation plan in Thailand. It will provide the proper value of earthquake level for seismic design of buildings and infrastructure. Moreover, it will be used to prepare proper resources such as the number of officers and equipments required for earthquake mitigation in each area in Thailand. It will be also used for specifying the earthquake insurance premium.

2. EARTHQUAKE CATALOG

The earthquake catalog contains instrumental records of past earthquakes. It is one of the most important tools used for interpreting seismicity and developing a seismic hazard map. The earthquake catalog containing a longer period of earthquake data generally represents a more complete image of seismicity and increases the accuracy of the seismic hazard map.

2.1 Compilation

The earthquake catalog in this project was originated from 4-year research, data compilation, and interpretation efforts of the Southeast Asia Association of Seismology and Earthquake Engineering (Nutalaya, 1985). The catalog contains the instrumental data of earthquake from 1912 to 1983 within boundary of 5^{o}N to 25^{o}N and 90^{o}E to 110^{o}E. The instrumental record was compiled from several sources, e.g. International Seismological Summary (ISS) (1914-1963), International Seismological Center (ISC) (1964-1980), Thai Meteorological Department (TMD) (1976-1983) and U.S. Geological Survey (USGS) (1975-1982).

Under a research project entitled "Assessment and Mitigation of Earthquake Risk in Thailand (Phase I)", the earthquake catalog was extended by adding the instrumental records from TMD (1984-2002) within 0^{o}N to 30^{o}N and 88^{o}E to 110^{o}E.

In this project, we updated the catalog by adding the instrumental records from 2003 to 2007 from TMD and USGS/NEIC (National Earthquake Information Center) Preliminary Determination of Epicenters on-line catalogue (http://neic.usgs.gov). The earthquake data from 1977 to 2007 from on-line USGS scientific data were also added to the catalog (http://earthquake .usgs.gov/research/topic). The original source of these data is the Harvard Seismological Group of Harvard University. Finally, we obtained earthquake catalog containing the earthquake data from 1912 to 2007 within 0^oN to 30^oN and 88^oE to 110^oE. Sample data from the final updated earthquake catalogue are shown in Table 1.

Table 1. Sample data from the final updated earthquake catalogue

No	Source	YR	MO	DA	HR	MN	SEC	LAT ^{o}	LONG ^{o}	DEPTH km	m_b	M_s	M_L	M_w
1	USGS	1978	06	07	10	26	19.9	6.34	94.15	33	5.0	4.5	-	-
2	ISC	1978	06	07	10	26	19.0	6.29	94.11	25	5.1	4.5	-	-
3	HFS	1978	06	07	10	26	8.0	5.00	94.00	-	5.3	-	-	-
4	MOS	1978	06	07	10	26	18.0	6.06	94.29	33	5.6	4.5	-	-
5	USGS	1980	05	06	22	23	20.2	22.15	94.22	167	4.0	-	-	-
6	ISC	1980	05	06	22	23	20.0	22.30	94.12	167	4.0	-	-	-
7	TMD	1980	05	07	15	38	58.5	14.21	96.75	10	-	-	3.9	-
8	TMD	1980	05	14	08	47	4.0	22.16	98.92	14	-	-	4.6	-
9	ISC	1980	05	14	08	47	10	22.20	98.70	33	4.2	-	-	-
10	ISC	1980	05	16	19	00	8.3	22.71	96.22	33	4.5	-	-	-
11	TMD	1980	05	20	13	19	31.1	24.29	93.14	33	-	-	5.1	-
12	USGS	1980	05	20	13	19	52.2	23.76	94.31	85	4.9	-	-	-
13	ISC	1980	05	20	13	19	51.9	23.72	94.20	83	4.8	5.4	-	-
14	MOS	1980	05	20	13	19	42.4	23.22	94.61	33	5.2	-	-	-
15	PEK	1980	05	20	13	19	54	23.90	94.20	-	4.7	-	-	-
16	ISC	1980	05	25	22	57	6.9	8.18	92.72	55	4.1	-	-	-
17	USGS	1980	05	26	11	37	30.5	11.07	92.7	65	4.9	-	-	-
18	ISC	1980	05	26	11	37	30.6	11.04	92.97	68	4.7	4.1	-	-
19	MOS	1980	05	26	11	37	25.8	10.92	93.22	33	5.1	-	-	-
20	PEK	1980	05	26	11	37	26.0	11.00	92.80	-	-	4.7	-	-

2.2 Magnitude Conversion

Different magnitudes scales were reported for each earthquake event in the final earthquake catalog depending on its original source. For example, the surface wave magnitude (M_s) and the short period P-wave magnitude (m_b) are commonly used in the data from USGS and ISC. While the local magnitude (M_L) is reported by TMD, and the moment magnitude (Mw) is reported in the Harvard catalog.

For the catalog to be usable for developing seismic hazard map, it is necessary to convert all earthquake events to a single magnitude scale. In this project, we choose to convert all magnitude scales to be moment magnitude (M_w) by a set of magnitude conversion equations as shown in Table 2.

Table 2. Magnitude conversion relations used in the study

Magnitude	Magnitude Range	Magnitude Conversion Relation	Reference
M_S	$3.0 \leq M_S \leq 6.1$	$M_W = 0.67\ M_S + 2.07$	Scordilis (2006)
	$6.2 \leq M_S \leq 8.2$	$M_W = 0.99\ M_S + 0.08$	Scordilis (2006)
m_b	$3.5 \leq m_b \leq 6.2$	$M_W = 0.85\ m_b + 1.03$	Scordilis (2006)
	$6.3 \leq m_b \leq 7.3$	$M_W = 1.46\ m_b - 2.42$	Sipkin (2003)
M_L	$M_L \leq 6$	$M_W = M_L$	Heaton (1986)

In cases where earthquake event is reported in both m_b and M_s, we choose M_s over m_b then convert M_s to M_w. The reason for choosing M_s over m_b, m_b was calculated based on P-wave in the first five-second which it is observed sometimes that the big earthquake wave which controls the earthquake magnitude comes later.

In cases where the earthquake event is reported in both M_L and m_b, or M_L and M_S, we choose m_b & M_S over M_L. We then convert m_b & M_S to M_w. This is because M_L calculated from different region cannot be compared to each other. In order to convert M_L to the other magnitude scales, it is necessary to provide the local magnitude conversion relation.

After the magnitude conversion, we remove the duplicate entries (from different data sources) to a single entry for each earthquake magnitude. The catalog of unduplicated event shows 16,303 earthquake records with magnitude greater than or equal to 5.

2.3 Declustering

In the earthquake source model, we assumed that the earthquake sequence can be modeled as a Poisson distribution (time-independent). Therefore, it is required that each earthquake entry in the catalog must be free from each other. The earthquake catalog is then declustered to remove dependent events such as foreshocks or aftershocks using the routines of Gardner and Knopoff (1974). Gardner and Knopoff identified duration, T, and dimension, L, as functions of mainshock magnitude, M, for a set of earthquake data, and fit least-upper-bound envelopes to the data of the form: log T or log L = aM + b. Following each earthquake in the chronologically ordered catalog, we scan for events in a [T(M), L(M)] window. If there is an event with magnitude less than M, it is deleted as a foreshock or aftershock. If there is an event with magnitude more than M, the original earthquake is deleted as a foreshock.

Declustering eliminates about 62 percent of the events in the catalogue. The final declustered catalog shows 6136 earthquake events with Mw greater than or equal to 5 in the study region from 1912 to 2007. These earthquake data are plotted in Figures 1-5.

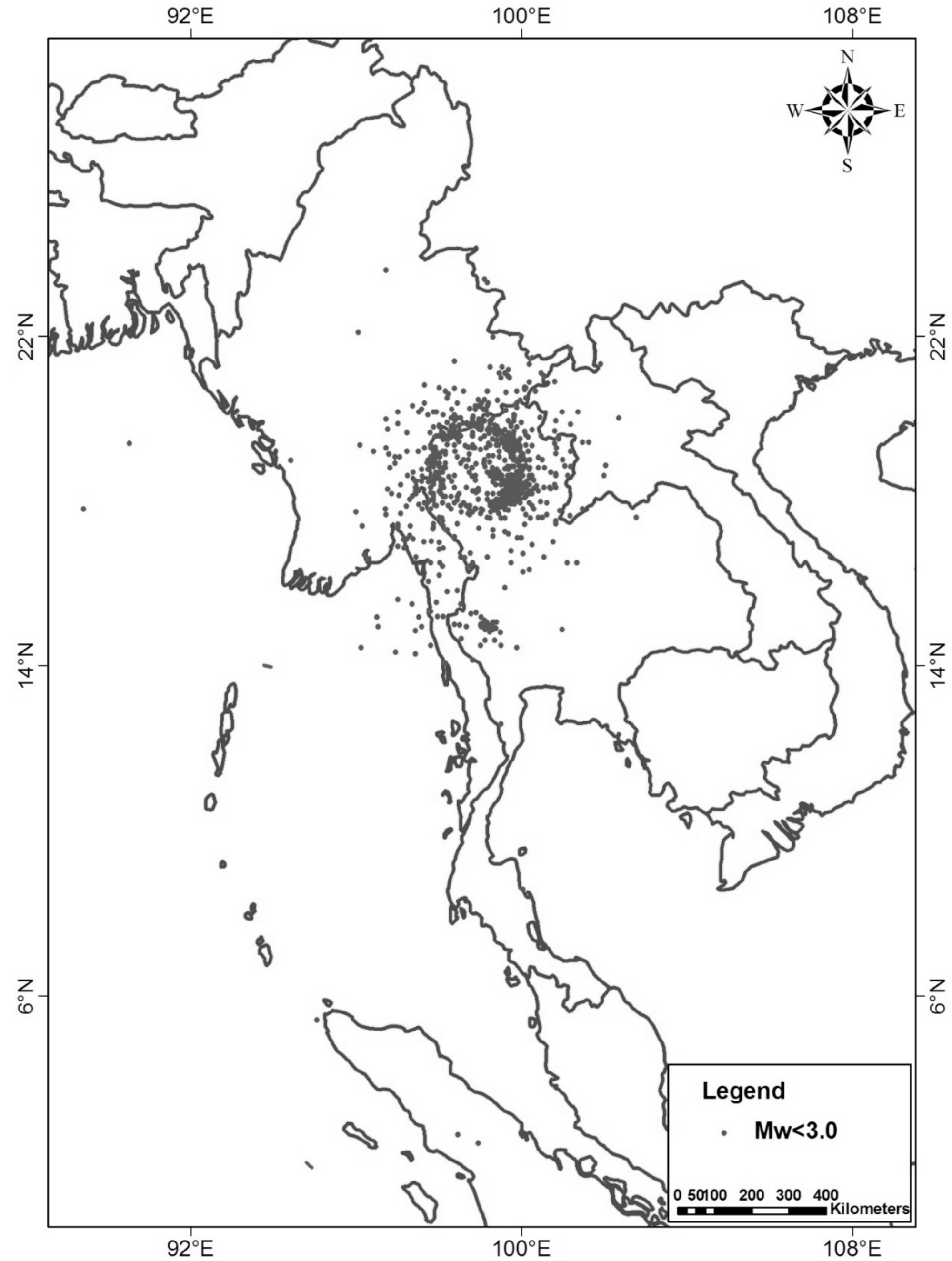

Figure 1: Earthquakes with magnitude lower than 3.0 in the study region from 1912 to 2007

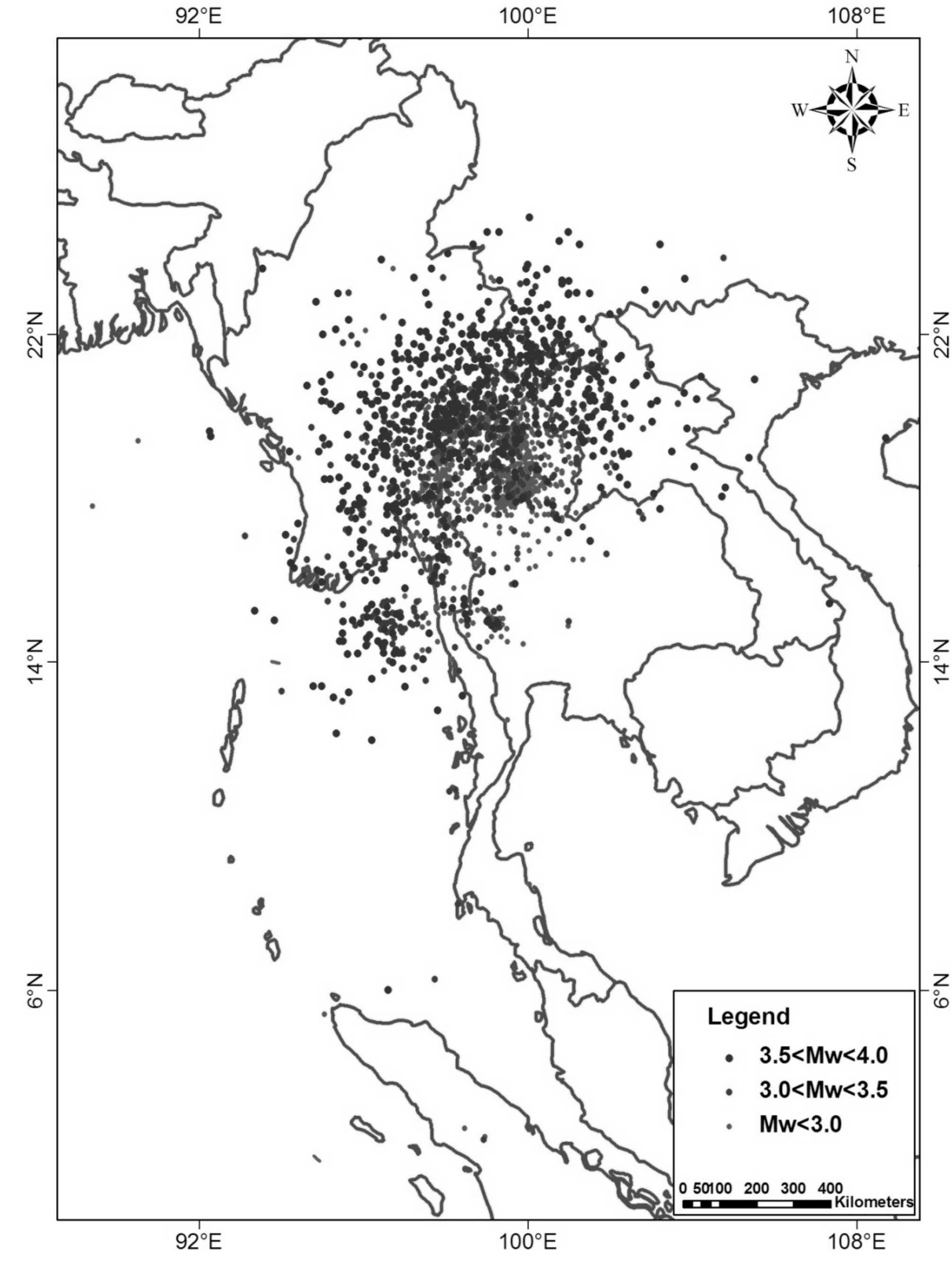

Figure 2: Earthquakes with magnitude lower than 4.0 in the study region from 1912 to 2007

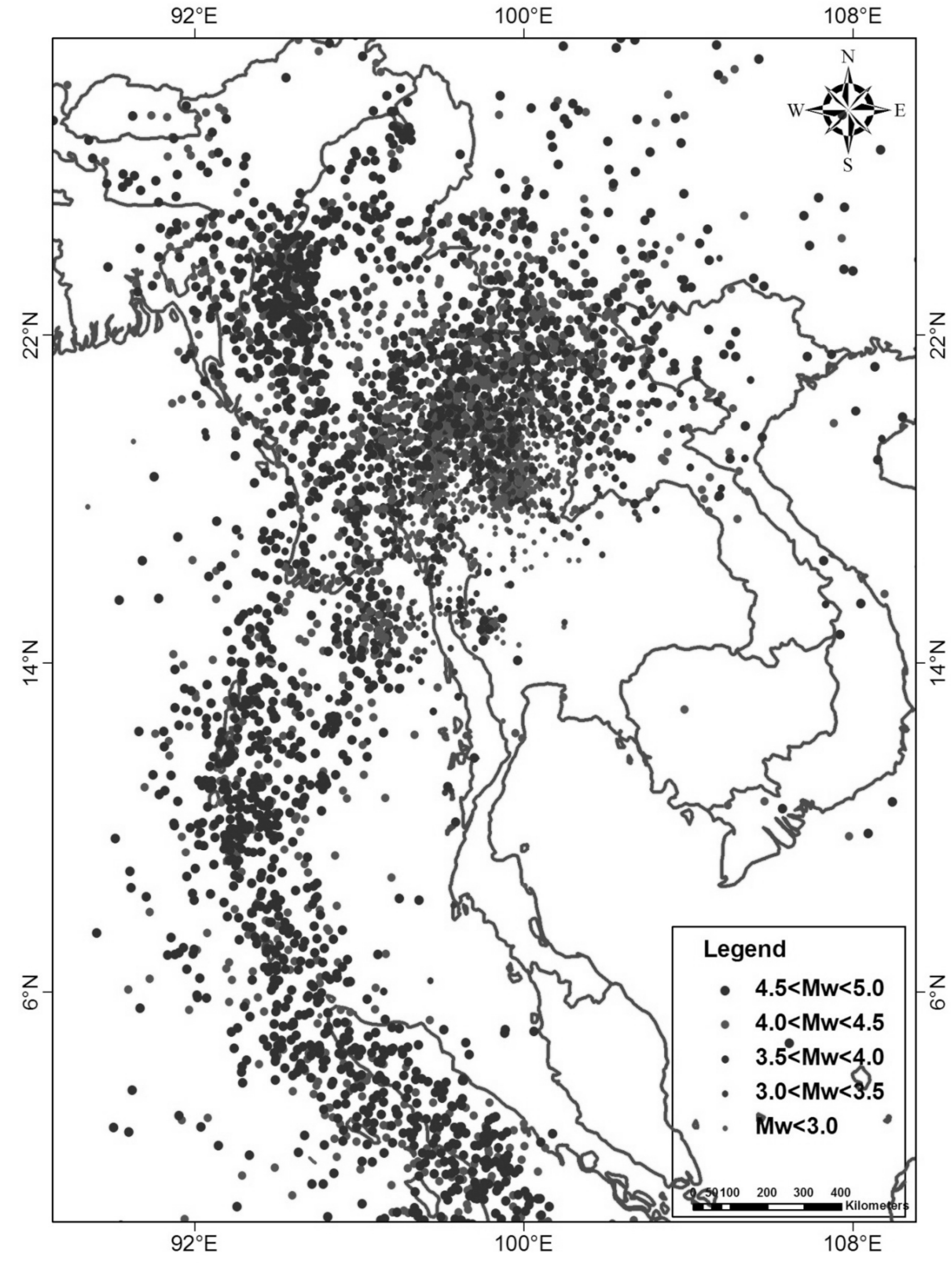

Figure 3: Earthquakes with magnitude lower than 5.0 in the study region from 1912 to 2007

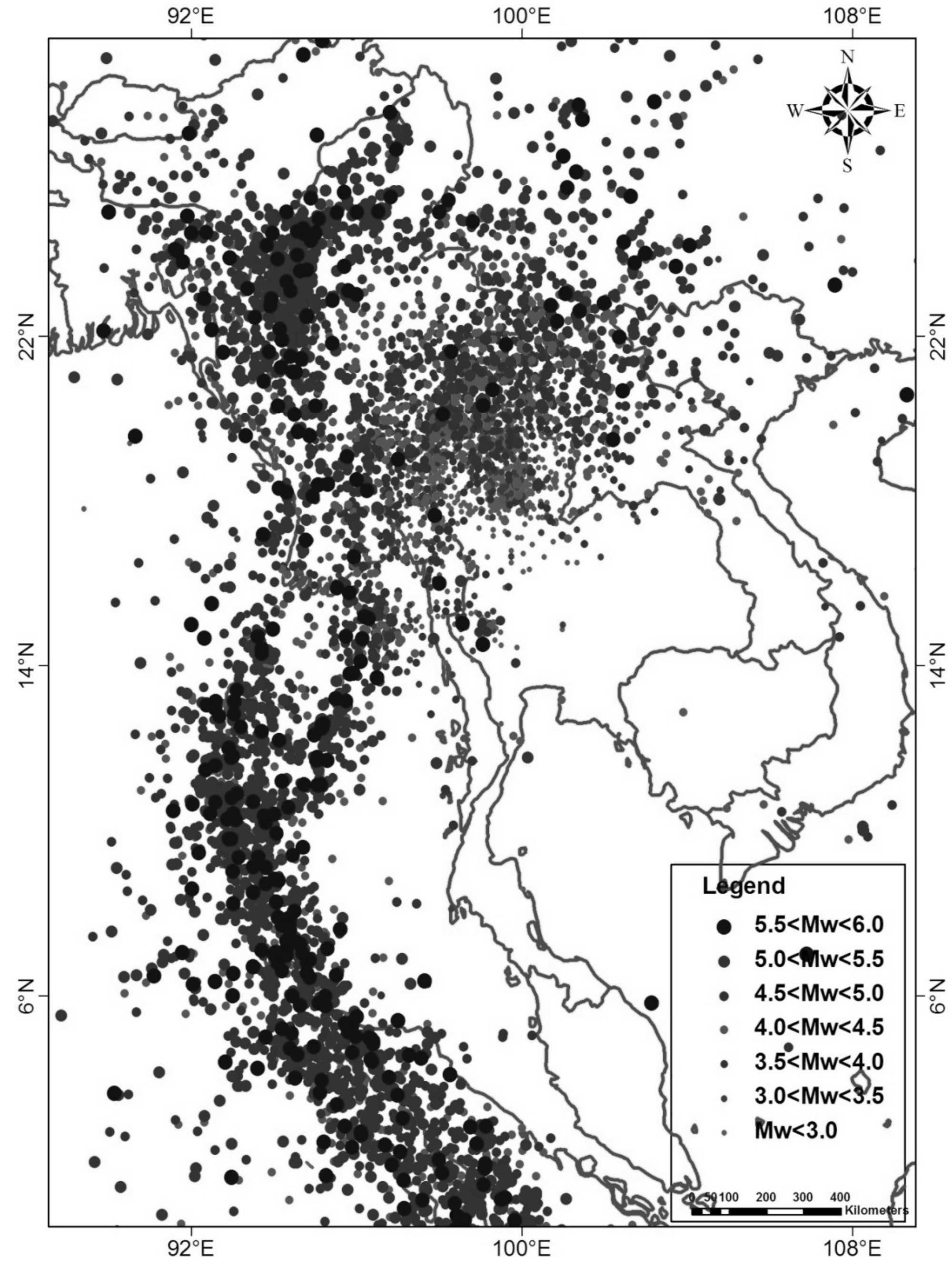

Figure 4: Earthquakes with magnitude lower than 6.0 in the study region from 1912 to 2007

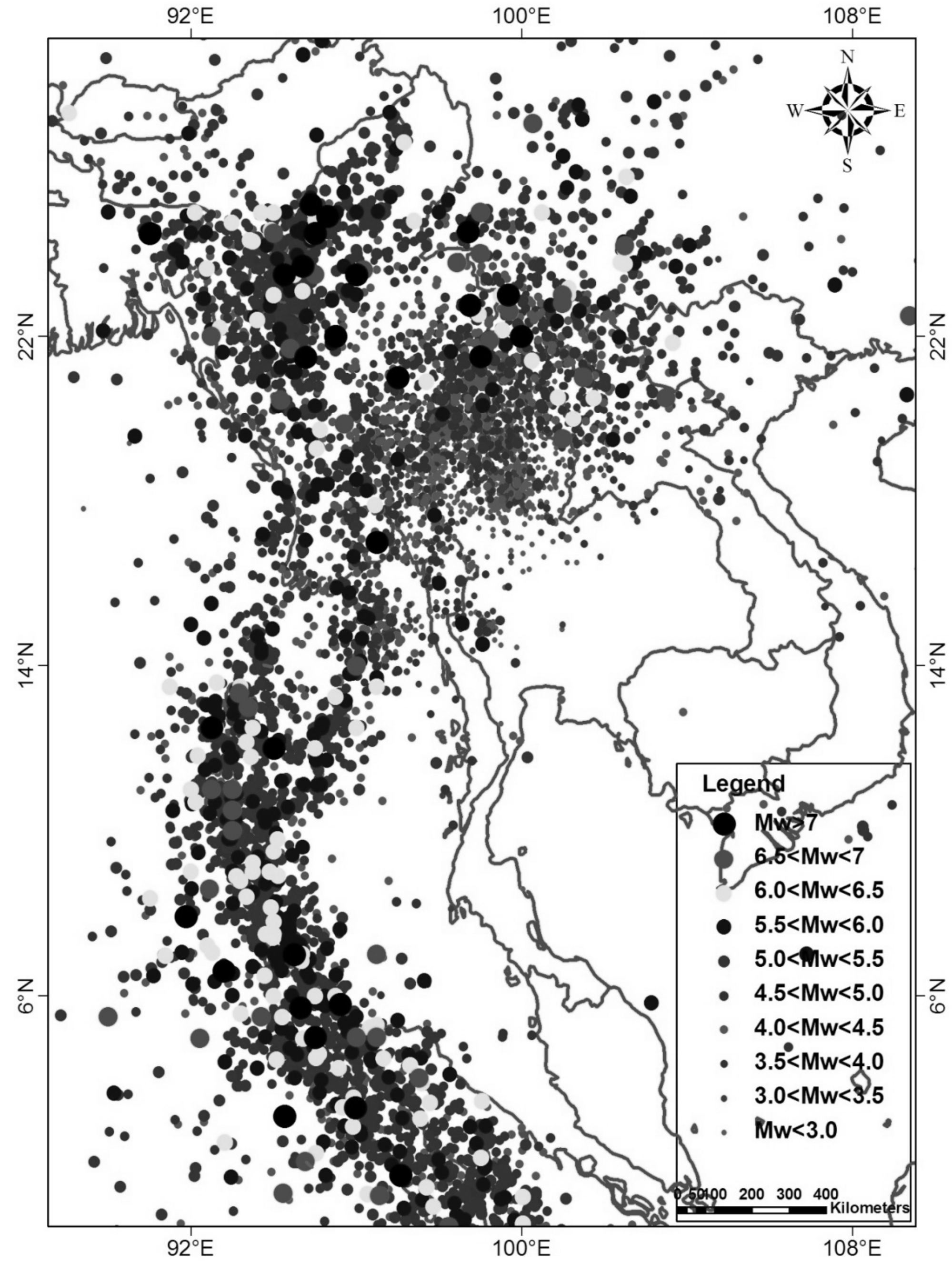

Figure 5: All earthquakes in the study region from 1912 to 2007

2.4 Catalog Completeness

Completeness of the earthquake catalog defines the times interval for earthquake events in a certain magnitude range that is completely recorded. Completeness of earthquake catalog is different for each magnitude range and each location depending on the quality of seismographic network in that area. The earthquake data in the catalog that fail to correct the data incompleteness cannot be used in the earthquake source model because 1) this data cannot be guaranteed to follow the Poison distribution assumption and 2) this data may result in underestimation of the mean rate of earthquake occurrence.

The completeness characteristic of the earthquake catalog in this project can be observed from Figure 6 which shows the plot between moment magnitude (M_w) and year of record. It can be seen that, as time passes, the smaller and smaller earthquakes can be detected. This is because the seismographic network has been continually developed in Thailand. It has been observed that the earthquake with magnitude less than 5.0 can be detected in 1962 which is the year that the seismographic network was drastically improved.

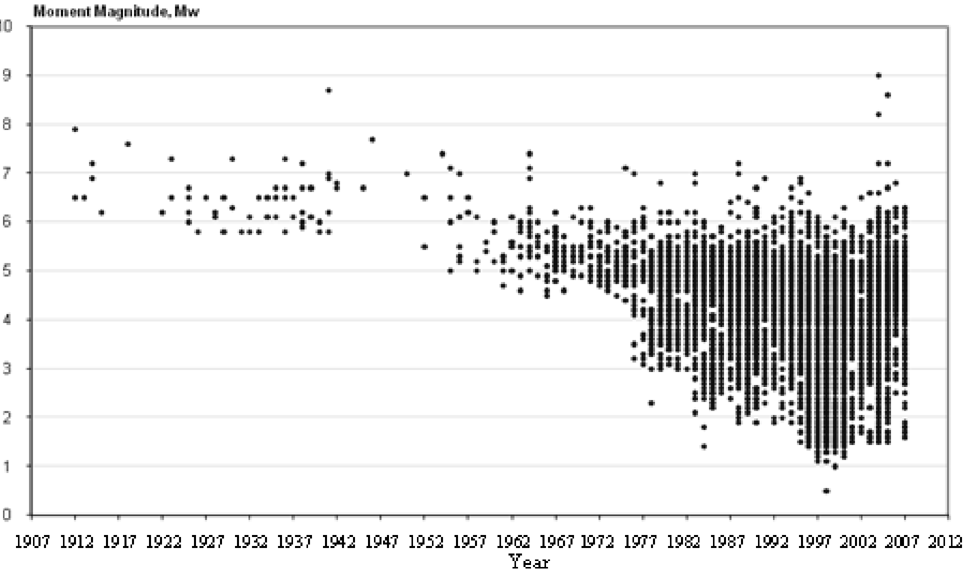

Figure 6: Distribution of earthquake data (Moment Magnitude, M_w) according to the occurrence year in the study area

Two methods were employed for completeness analysis of the catalog: (1) the Visual Cumulative method (CUVI) (Tinti and Mulargia, 1985), & (2) the Stepp method (Stepp, 1973). We divide the study region into five zones – 3 subduction zones (SD-A, SD-B, SD-C), Thailand and surrounding zone (BG-I), and the remaining zone (BG-II). These five zones are shown in Figure 7.

In CUVI method, the completeness times for different magnitude ranges (says events greater than reference value, M_{wref}) can be determined from the plot between the cumulative number of events and time for events with the magnitude between M_{wref} and $M_{wref}+0.5$. The example of completeness analysis by CUVI method is shown in the plots for zone BG-I (Figure 8 and 9). From each figure, the completeness time for each magnitude range is considered from the time period that the plot has a constant slope (black line).

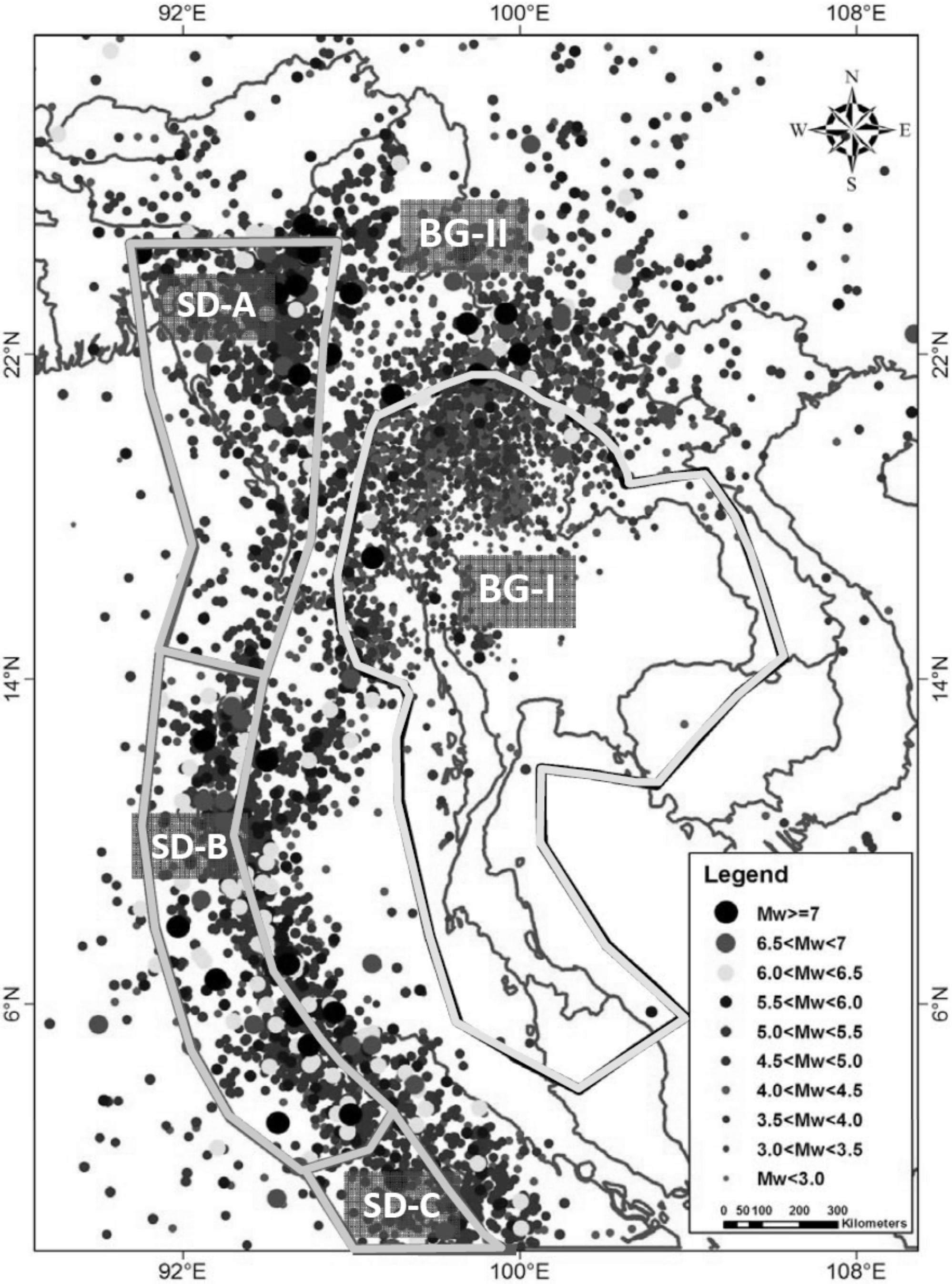

Figure 7: Background seismicity zones (BG-I and BG-II) and subduction zones (SD-A, SD-B, and SD-C)

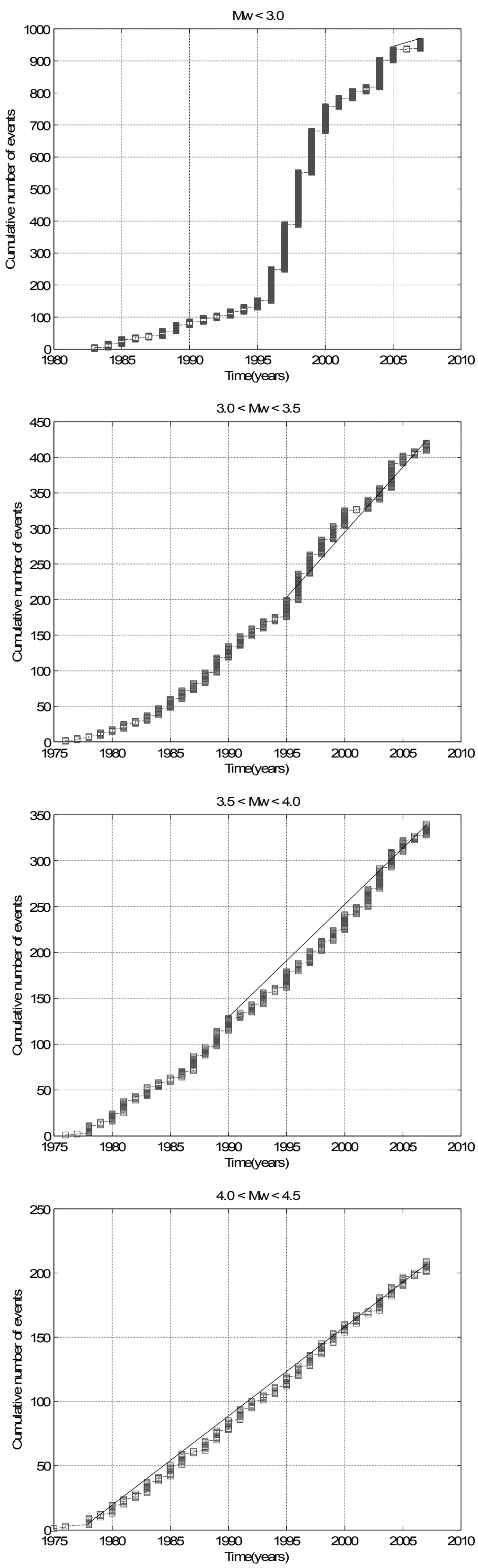

Figure 8: Example of completeness analysis of the earthquake catalog for Mw<4.5 by CUVI method in BG-I zone

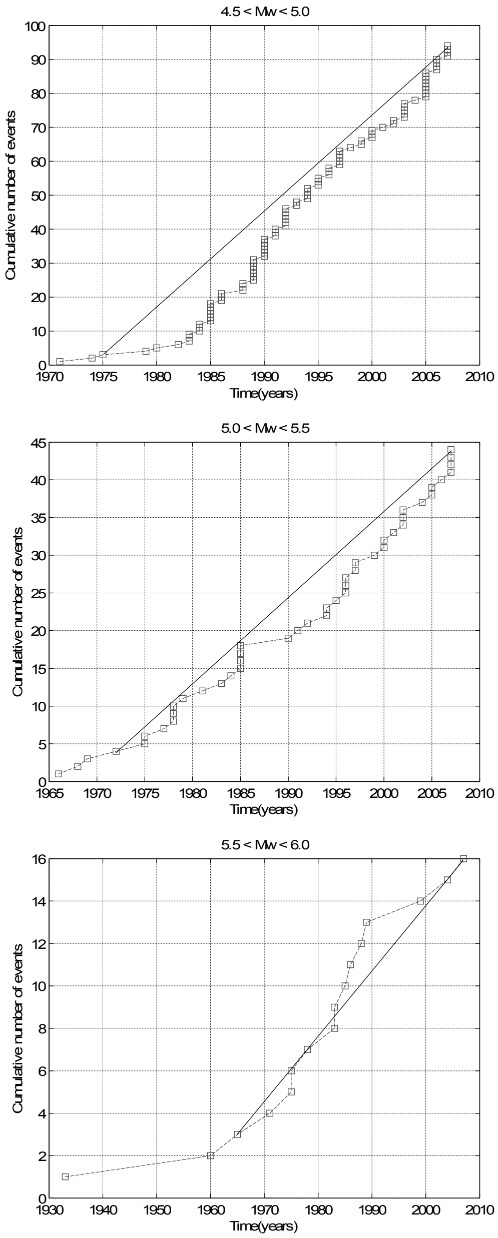

Figure 9: Example of Completeness analysis of the earthquake catalog for Mw>4.5 by CUVI method in BG-I zone

The Stepp method uses the statistical procedures to assess the completeness times of the reported magnitudes, which assume the earthquake sequence in catalog can be modeled as a Poisson distribution. If *k1, k2, k3, ... k_n* are the number of events per unit time interval, then :

$$\lambda = \frac{1}{n}\sum_{i=1}^{n} k_i$$

and its variance is $\sigma^2=\lambda/n$, where λ is the average of the occurrences in the period T and *n* equals the number of unit time intervals. If unit time is one year, $\sigma_\lambda=\lambda^{1/2}/T^{1/2}$ as the standard deviation of the estimate of the mean where *T* is the sample length in years. The earthquake data in the catalog is used to calculate standard deviation (σ_λ) for each sample years (*T*), and log(σ_λ) and log(*T*) is plotted as shown in Figure 10. The completeness time is determined from the portion of the line with $T^{1/2}$. The completeness time from Stepp method for zone BG-1 and BG-2 are summarized in Table 3. It can be observed that there is a good correlation between completeness time obtained from CUVI and Stepp method. However, we chose the result from CUVI method as we feel less subjective in determining completeness range. The summary of the completeness period for the earthquake catalog is shown in Table 3 for BG-I and BG-II and Table 4 for subduction zones, respectively.

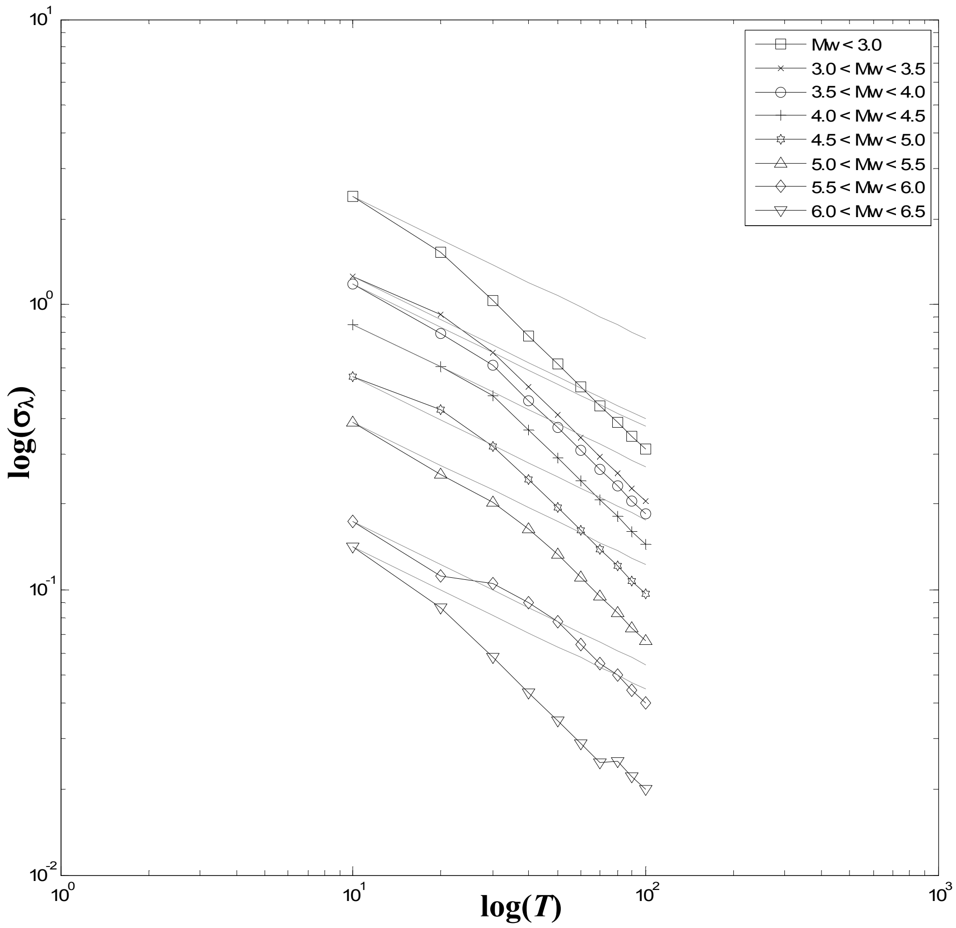

Figure 10: Example of Completeness analysis of the earthquake catalog by Stepp method in BG-I zon

Table 3: Completeness period for earthquake catalog in BG-I and BG-II zone

Magnitude Range	**Zone BG-I**			**Zone BG-II**		
	Years of completeness data	**Time period of completeness data** *(years)*	**Number of Earthquakes** *(events)*	**Years of completeness data**	**Time period of completeness data** *(years)*	**Number of Earthquakes** *(events)*
$M < 3.0$	2005-2007	2	60	2005-2007	2	3
$3.0 < M < 3.5$	1995-2007	12	245	1995-2007	12	87
$3.5 < M < 4.0$	1990-2007	17	226	1995-2007	12	163
$4.0 < M < 4.5$	1977-2007	30	206	1990-2007	17	375
$4.5 < M < 5.0$	1975-2007	32	91	1982-2007	25	709
$5.0 < M < 5.5$	1972-2007	35	41	1972-2007	35	453
$5.5 < M < 6.0$	1964-2007	43	15	1964-2007	43	135
$6.0 < M < 6.5$	1930-2007	77	4	1930-2007	77	53
$6.5 < M < 7.0$	1912-2007	95	1	1912-2007	95	24
$M \geq 7.0$	1912-2007	95	1	1912-2007	95	12

Table 4: Completeness period for earthquake catalog in subduction zones

Magnitude Range	**Burma Zone**			**Northern Sumatra Zone**			**Southern Sumatra Zone**		
	Years of completeness data	**Time period of completeness data** *(years)*	**Number of Earthquakes** *(events)*	**Years of complete data**	**Time period of completeness data** *(years)*	**Number of Earthquakes** *(events)*	**Years of completeness data**	**Time period of completeness data** *(years)*	**Number of Earthquakes** *(events)*
$5.00<M<5.49$	1964-2007	43	203	1960-2007	47	198	1960-2007	47	58
$5.50<M<5.99$	1962-2007	45	60	1950-2007	57	60	1950-2007	57	16
$6.00<M<6.49$	1955-2007	52	15	1930-2007	77	30	1930-2007	77	4
$6.50<M<6.99$	1925-2007	82	7	1925-2007	82	8	1925-2007	82	2
$M \geq 7.00$	1912-2007	95	6	1912-2007	95	7	1912-2007	95	1

3. MODELLING OF EARTHQUAKE SOURCES

To properly describe the complex earthquake sources in the region, they are modeled as a combination of background seismicity, subduction area sources, and crustal faults. They are described in more detail in the following.

3.1 Background seismicity model

We use the background seismicity model to represent random earthquakes in the whole study region except subduction zones. The model accounts for all earthquakes in areas with no mapped faults and for smaller earthquakes in areas with mapped faults.

There are two different approaches to model background seismicity. The first and traditional approach is to divide the region into many areas, where a uniform rate of seismicity is assumed for each area. Earthquakes are assumed to occur randomly at any location with an equal probability in each area. Although this approach has been commonly and widely used in the past, it has many drawbacks. Among these, the most serious drawback is that the seismic hazard assessment results can be significantly affected by the delineation of areas, which is heavily dependent on the subjective judgment of the hazard analyst.

To resolve this drawback, the second approach—spatially smoothed seismicity model—has been recently proposed for modeling background seismicity. In this approach, it is not necessary to divide the region into many areas. One large area may be used, but the rate of seismicity is assumed to vary from place-to-place within the area. The rate of seismicity is determined by first overlaying a grid with spacing, say, 0.1^o in latitude and 0.1^0 in longitude onto the region, and counting the number of earthquakes with magnitude greater than a reference value (M_{ref}) in each grid cell. The rate of seismicity is computed by dividing the number of earthquakes by the time period of earthquake data. The rate is then smoothed spatially by a Gaussian-function moving average. By this approach, the spatially varied seismicity can be modeled without being affected by the subjectivity of the hazard analyst.

This spatially smoothed background seismicity model was used by the US Geological Survey in the development of seismic hazard maps in Central and Eastern United States (Frankel, 1995).

We adopt this spatially smoothed background seismicity model in this study. The whole study region is divided into 5 source zones: BG-I, BG-II, SD-A, SD-B, and SD-C (Figure 7). The zones SD-A, SD-B, and SD-C are subduction zones, which will be described in detail later. The zone BG-I is a background seismicity zone covering Thailand and surrounding areas, and the zone BG-II is another background seismicity zone covering the remaining areas except the 3 subduction zones.

Earthquake data, particularly small earthquakes, in BG-I are much more completely recorded than those in BG-II (see Figure 1 to 5). This is due to the high earthquake detection capability of a fairly dense seismograph network in Thailand. Hence, the accuracy of estimated seismicity rate in BG-I can be significantly improved by including data of smaller earthquakes ($3.0 < M_W < 5.0$) in the seismicity rate calculation. This is important because the seismicity rate inside Thailand is somewhere between low to moderate. On the other hand, in BG-II only earthquake data with $M_W > 5.0$ can be used for computing the seismicity rate due to the incompleteness of small earthquake data. Nevertheless, lacking of small earthquake data is not a major problem because the seismicity rate in this zone is relatively high, so that the rate can be reliably estimated from moderate earthquakes. In addition, the influence of BG-II on the seismic hazard in Thailand is lower than that of BG-I.

We model the magnitude-dependent characteristic of seismicity rate in each background seismicity zone by a truncated exponential model (Gutenberg-Richter model):

$$\mathrm{Log}_{10}\, N(M_W) = a - b\, M_W \qquad (1)$$

Where $N(M_W)$ is the annual occurrence rate of earthquakes with magnitude greater than or equal to M_W, and a and b are the model parameters.

The b-value is assumed to be uniform throughout the whole background region. Hence, we used complete earthquake data with magnitude greater than 4.0 in both BG-I and BG-II to compute a single regional b value. The obtained regional b-value is 0.90, and this value is used for both BG-I and BG-II.

The a-value varies from place-to-place within each zone. It is computed by using a grid with spacing of in latitude and longitude and is spatially smoothed using a two-dimensional Gaussian moving average operator with a correlation distance parameter C. Earthquake data with $M_W > 3.0$ and C = 50 km are used for BG-I, while earthquake data with $M_W > 5.0$ and C = 75 km are used for BG-II. The resulted smoothed rate 10^a values are presented in Figures 11 and 12.

In the truncated GR models of both BG-I and BG-II, the minimum earthquake magnitude is set to 5.0 because earthquakes smaller than this level do not normally cause damage to buildings and structures. The maximum (upper bound) magnitude is set to 7.5 for BG-II to account for many large earthquakes in this zone as shown in Figure 7. On the other hand, in BG-I large earthquakes are accounted for by crustal faults (details are shown in crustal faults section), so the maximum magnitude is set to 6.5 to avoid the double-counting effect in this zone.

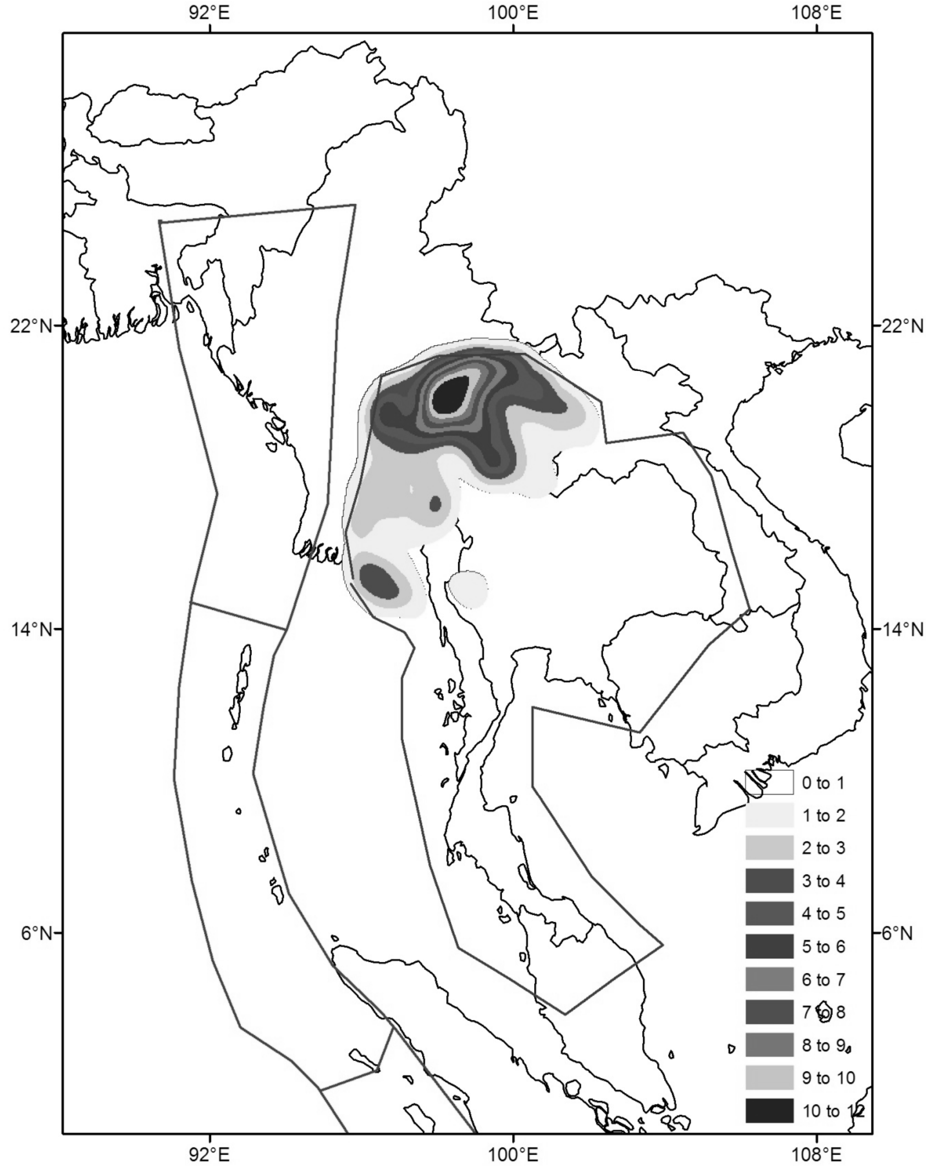

Figure 11: Map of Smooth 10^a values derived from M_w 3.0 and larger earthquakes in zone BG-I (correlation distance of 50 km)

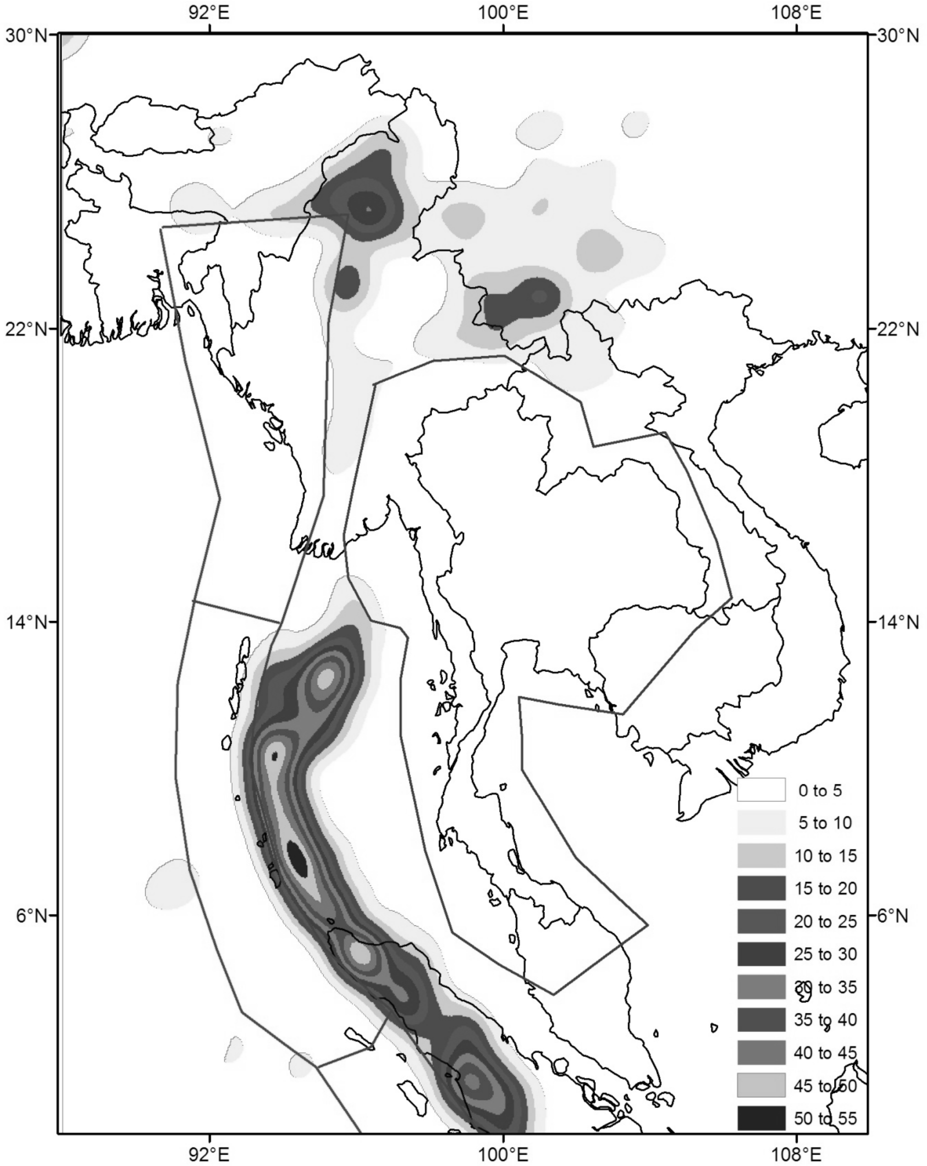

Figure 12:Map of Smooth 10^a values derived from M_w 5.0 and larger earthquakes in zone BG-II (correlation distance of 75 km)

3.2 Subduction zone model

As explained earlier, the megathrust Sunda subduction zone is divided into 3 sub zones based on seismicity characteristics: Burma (SD-A), Northern Sumatra-Andaman (SD-B), and Southern Sumatra (SD-C). Each sub zone is modeled as a seismic area source with a uniform rate of seismicity (the traditional area source model), and the magnitude-dependent characteristic of seismicity rate is modeled by a truncated GR model.

The calculations to identify GR model parameters (*a* and *b* values) are shown by Figures 13-15. The minimum earthquake magnitude in the GR model is set to 6.5 as the subduction zones are very far from Thailand. The maximum magnitude for zone SD-A is set to 8.1, which is equal to the maximum observed magnitude plus 0.5. The maximum magnitude for zone SD-B and SD-C is set to 9.2 as the 2004 Sumatra earthquake and the 2005 Nias earthquake has already demonstrated the capability of the zones to generate large mega thrust earthquakes.

SD-A : BURMA SUBDUCTION ZONE

Years of completeness data	Time period of completeness data *(years)*	Magnitude range	M	Number of earthquakes *(events)*	Annual occur. rate *(events/year)*	$N_{(M)}$ Cumulative rate *(events/year)*	$Log_{10} N_{(M)}$
1964-2007	43	5.00 - 5.49	5.0	203	4.7209	6.4912	0.8123
1962-2007	45	5.50 - 5.99	5.5	60	1.3333	1.7703	0.2480
1955-2007	52	6.00 - 6.49	6.0	15	0.2885	0.4370	-0.3595
1925-2007	82	6.50 - 6.99	6.5	7	0.0854	0.1485	-0.8282
1912-2007	95	> 7.00	7.0	6	0.0632	0.0632	-1.1996

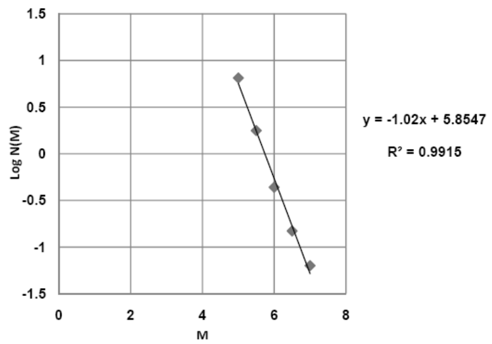

$Log_{10} N_{(M)} = a - b.M$

Where a = 5.854, b= 1.02

Lower bound Magnitude: 6.5
Upper bound Magnitude: 8.1

(Max observed Magnitude: 7.6)

Figure 13: Calculation sheet to determine the GR model parameters of subduction zone SD-A

SD-B : NORTHERN SUMATRA SUBDUCTION ZONE

Years of completeness data	Time period of completeness data *(years)*	Magnitude range	M	Number of earthquakes *(events)*	Annual occur. rate *(events/year)*	$N_{(M)}$ Cumulative rate *(events/year)*	$Log_{10} N_{(M)}$
1960-2007	*47*	*5.00 - 5.49*	*5.0*	*198*	*4.2128*	*5.8263*	*0.7654*
1950-2007	*57*	*5.50 - 5.99*	*5.5*	*60*	*1.0526*	*1.6135*	*0.2078*
1930-2007	*77*	*6.00 - 6.49*	*6.0*	*30*	*0.3896*	*0.5609*	*-0.2512*
1925-2007	*82*	*6.50 - 6.99*	*6.5*	*8*	*0.0976*	*0.1712*	*-0.7664*
1912-2007	*95*	*> 7.00*	*7.0*	*7*	*0.0737*	*0.0737*	*-1.1326*

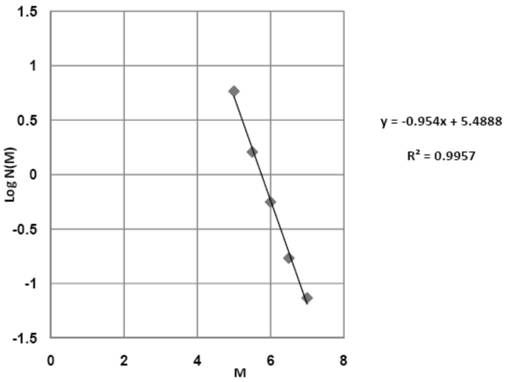

$Log_{10} N_{(M)} = a - b.M$

Where $a = 5.488$, $b = 0.954$

Lower bound Magnitude: 6.5
Upper bound Magnitude: 9.2

(Max observed Magnitude: 9.0)

Figure 14: Calculation sheet to determine the GR model parameters of subduction zone SD-B

SD-C : SOUTHERN SUMATRA SUBDUCTION ZONE

Years of completeness data	Time period of completeness data *(years)*	Magnitude range	M	Number of earthquakes *(events)*	Annual occur. rate *(events/year)*	$N_{(M)}$ Cumulative rate *(events/year)*	$Log_{10} N_{(M)}$
1960-2007	*47*	*5.00 - 5.49*	*5.0*	*58*	*1.2340*	*1.6016*	*0.2046*
1950-2007	*57*	*5.50 - 5.99*	*5.5*	*16*	*0.2807*	*0.3676*	*-0.4347*
1930-2007	*77*	*6.00 - 6.49*	*6.0*	*4*	*0.0519*	*0.0869*	*-1.0612*
1925-2007	*82*	*6.50 - 6.99*	*6.5*	*2*	*0.0244*	*0.0349*	*-1.4570*
1912-2007	*95*	*> 7.00*	*7.0*	*1*	*0.0105*	*0.0105*	*-1.9777*

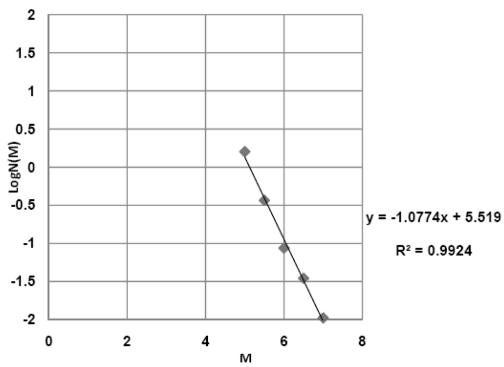

$Log_{10} N_{(M)} = a - b.M$

Where $a = 5.519$, $b = 1.077$

Lower bound Magnitude: 6.5
Upper bound Magnitude: 9.2

(Max observed Magnitude: 8.6)

Figure 15: Calculation sheet to determine the GR model parameters of subduction zone SD-C

A subduction earthquake in each zone is assumed to be created by a rupture along an inclined plane at the interface between two tectonic plates. The plane is 5 km deep at the left-hand-side zone boundary and is 50 km deep at the right-hand-side zone boundary. This assumption is based on a recent work on *'Teleseismic relocation and assessment of seismicity (1918-2005) in the region of the 2004 MW 9.0 Sumatra-Andaman and 2005 MW 8.6 Nias Island great earthquakes'* by E. Robert Engdahl and his co-workers, presented at the 6th General Assembly of the Asian Seismological Commission in Bangkok in 2006 (ASC2006).

3.3 crustal fault source model

Twenty-one crustal fault sources are modeled explicitly in this study as shown in Figure 16. Their important properties and parameters are illustrated by logic tree diagrams in Figures 17-37.

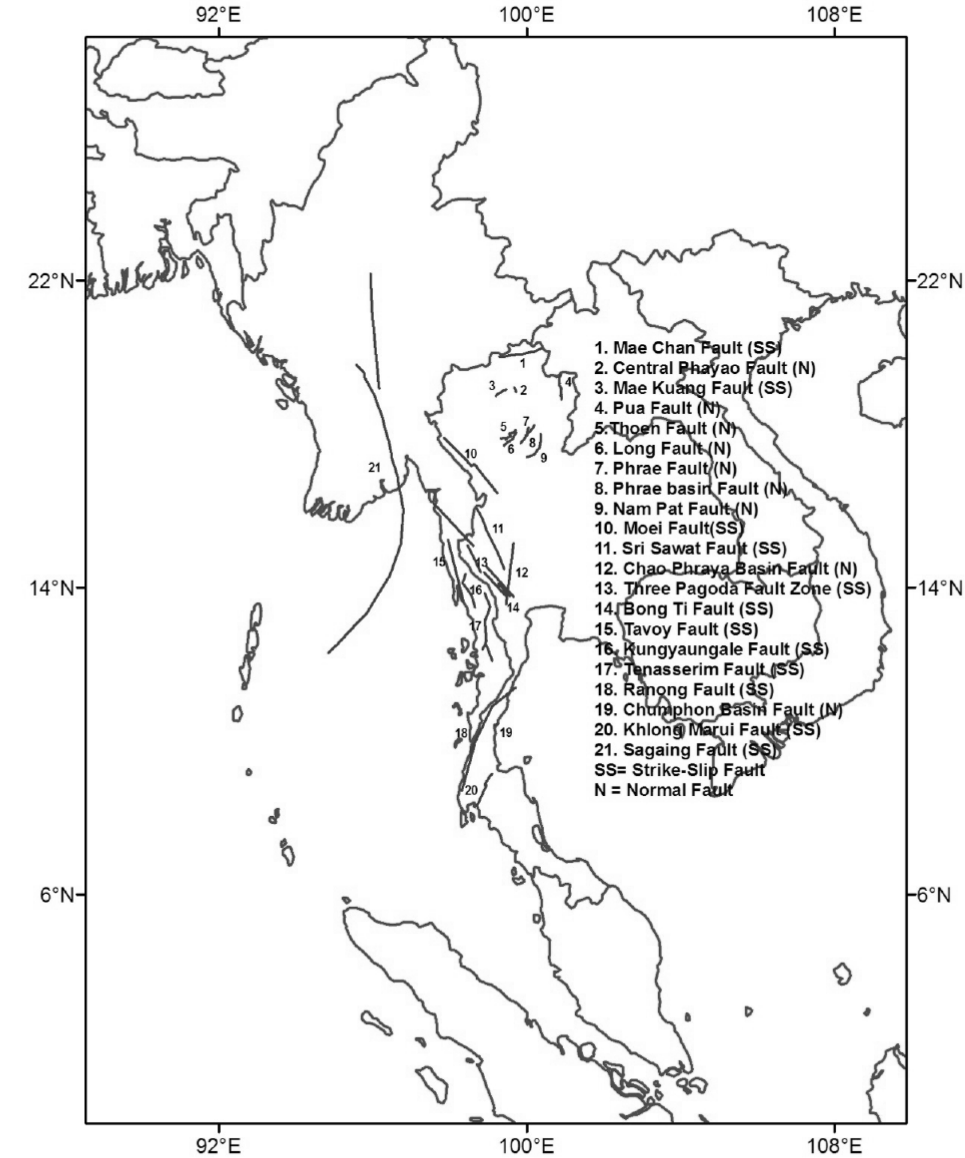

Figure 16: Map of crustal fault sources in and near Thailand considered in this study

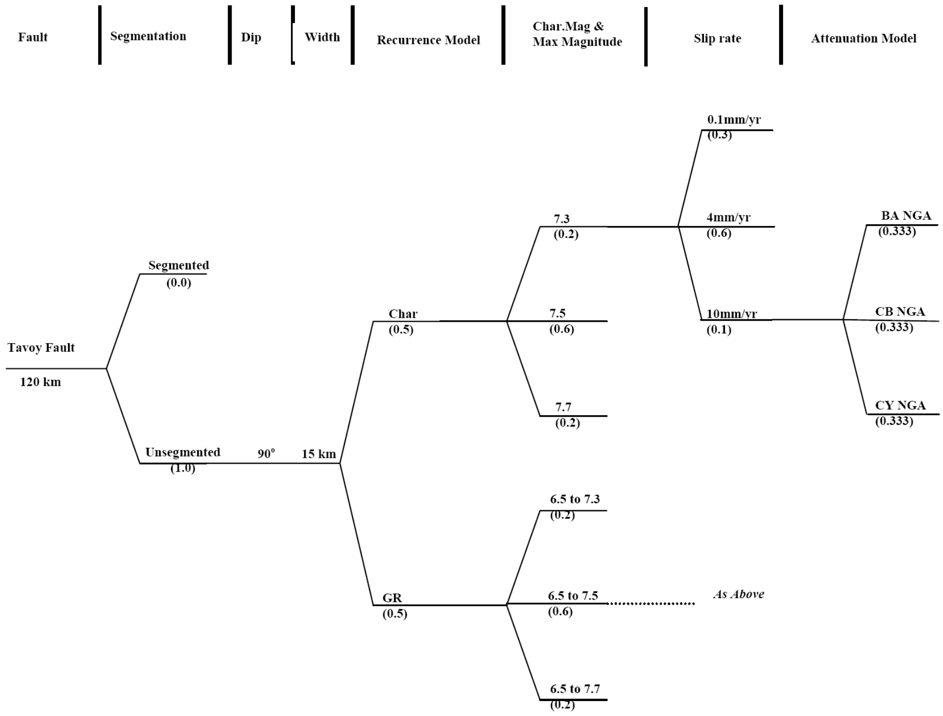

Figure 17: Logic tree diagram of Tavoy fault

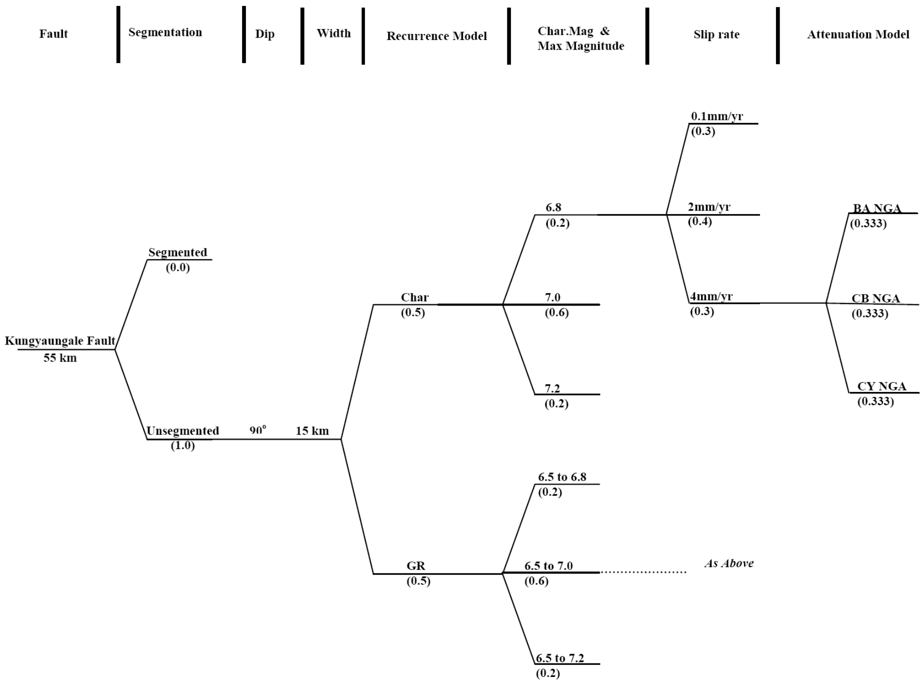

Figure 18: Logic tree diagram of Kungyaungale fault

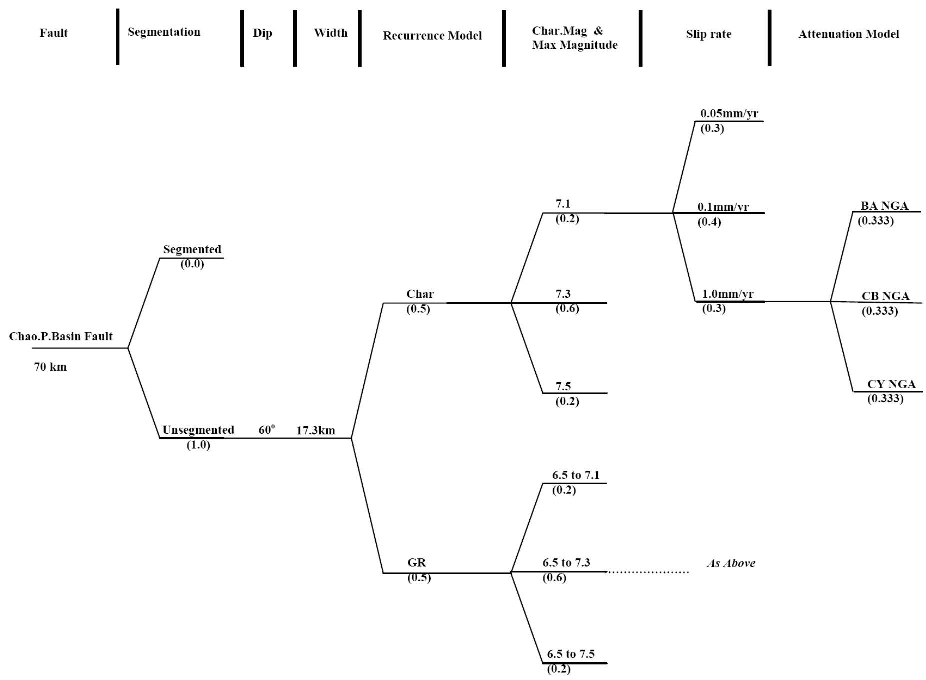

Figure 19: Logic tree diagram of Chao Phraya Basin fault

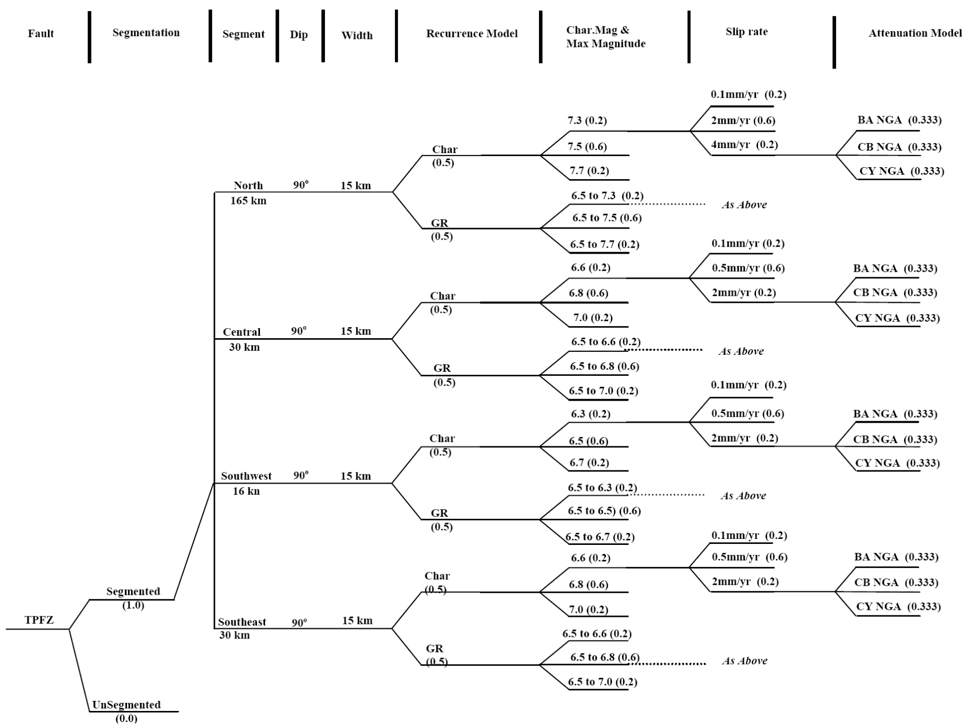

Figure 20: Logic tree diagram of Three Pagoda Fault Zone

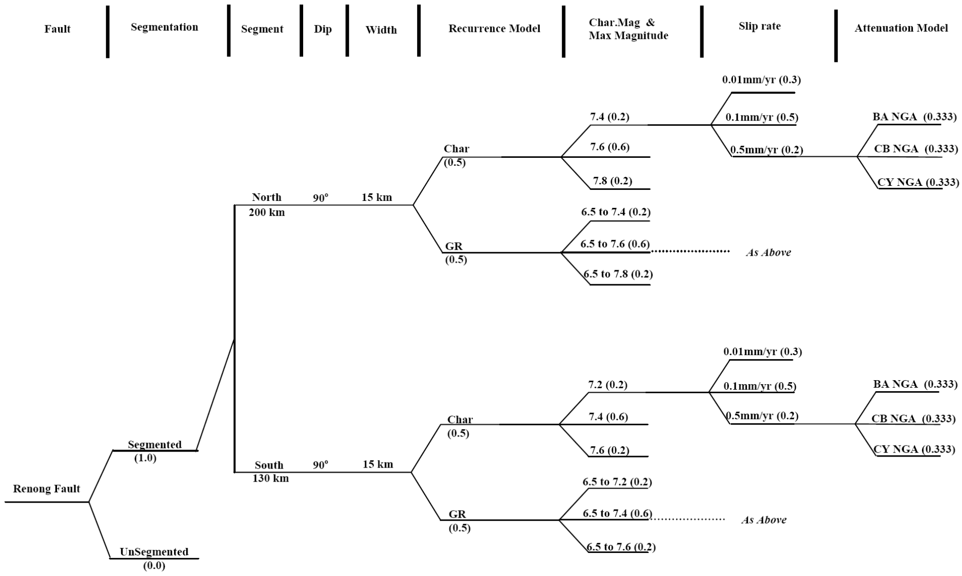

Figure 21: Logic tree diagram of Ranong fault

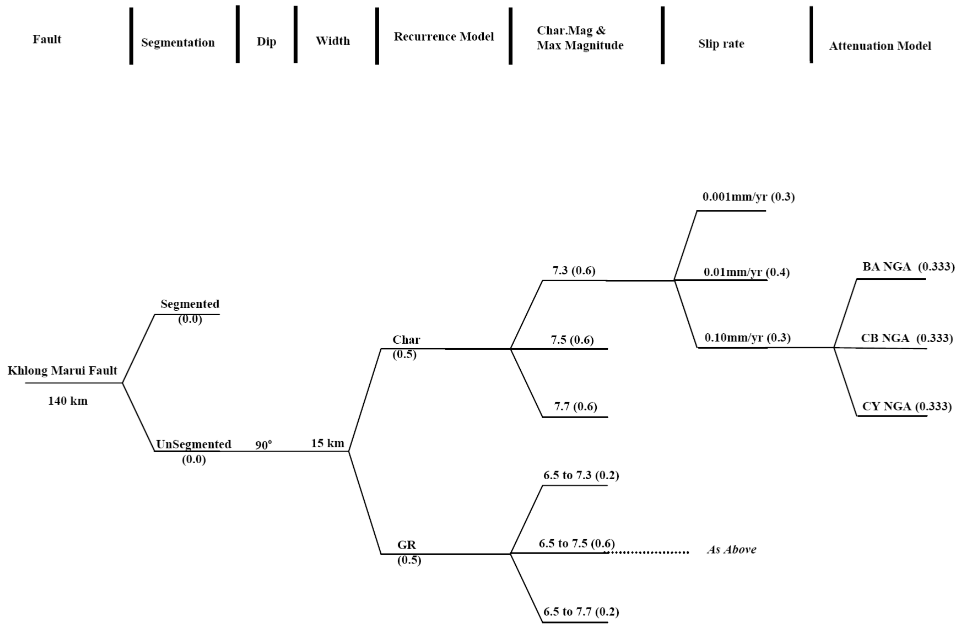

Figure 22: Logic tree diagram of Khlong Marui fault

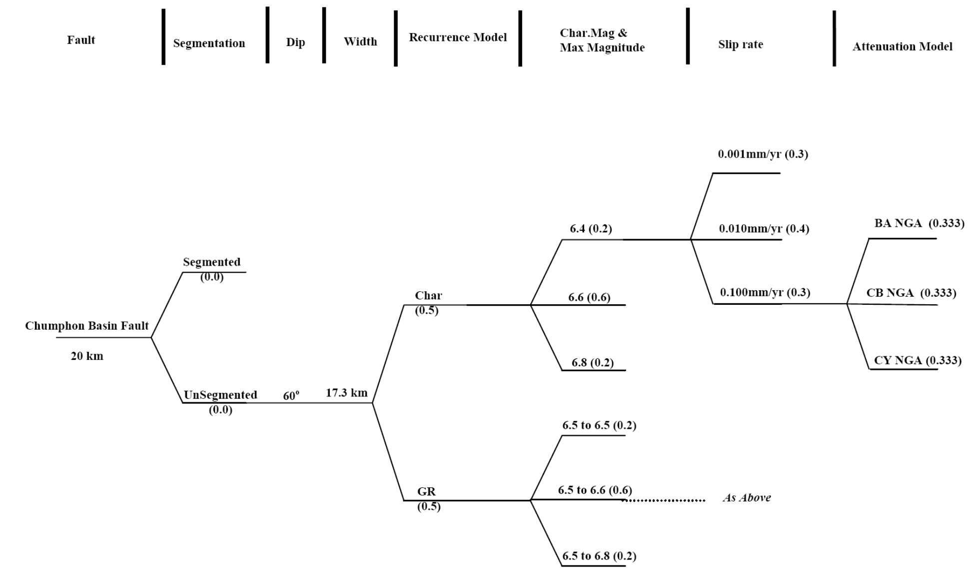

Figure 23: Logic tree diagram of Chumporn Basin fault

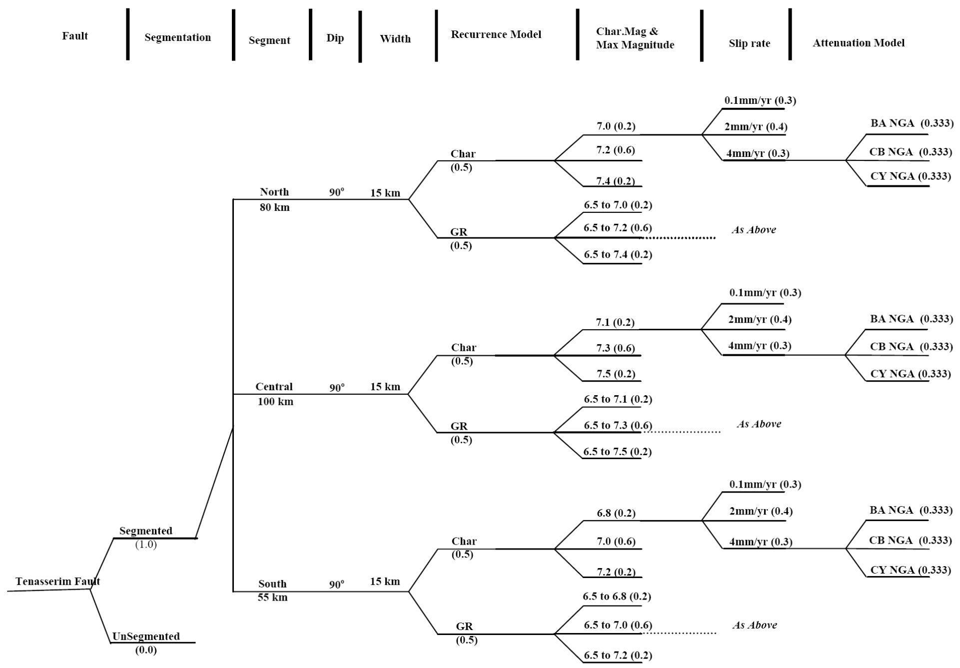

Figure 24: Logic tree diagram of Tenasserim fault

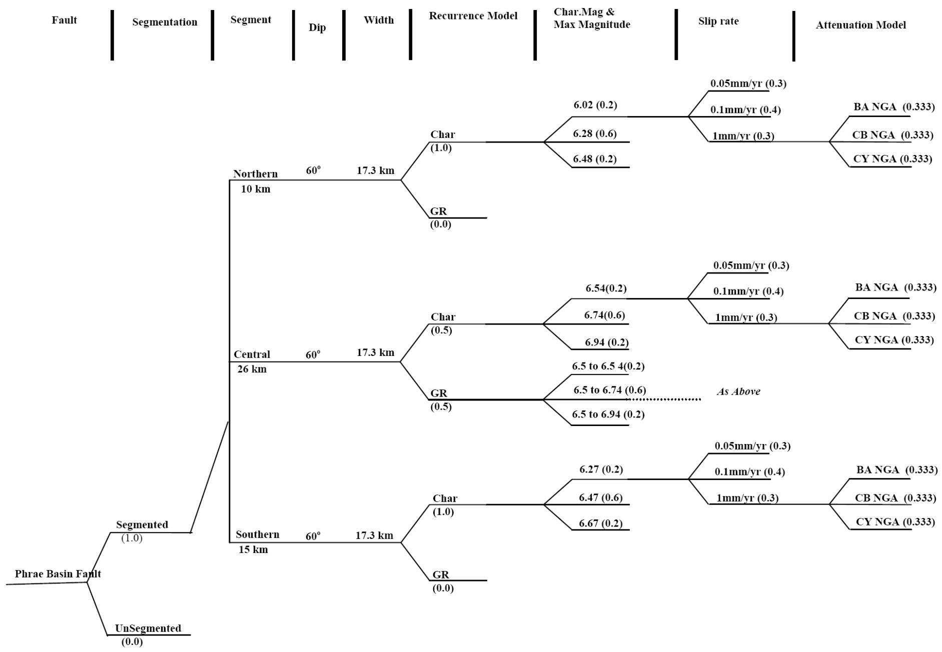

Figure 25: Logic tree diagram of Phrae Basin fault

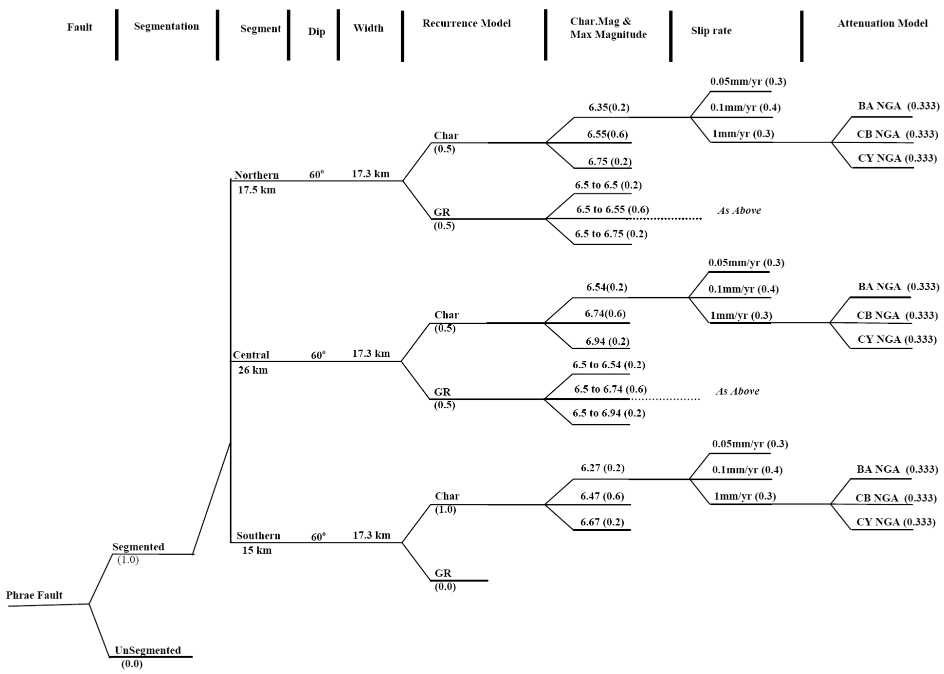

Figure 26: Logic tree diagram of Phrae fault

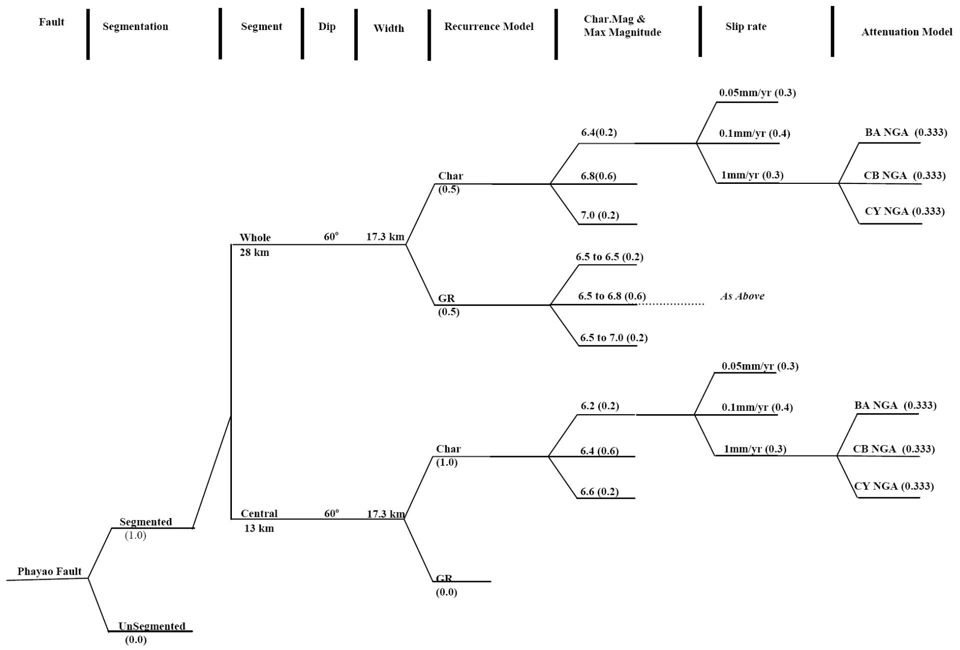

Figure 27: Logic tree diagram of Phayao fault

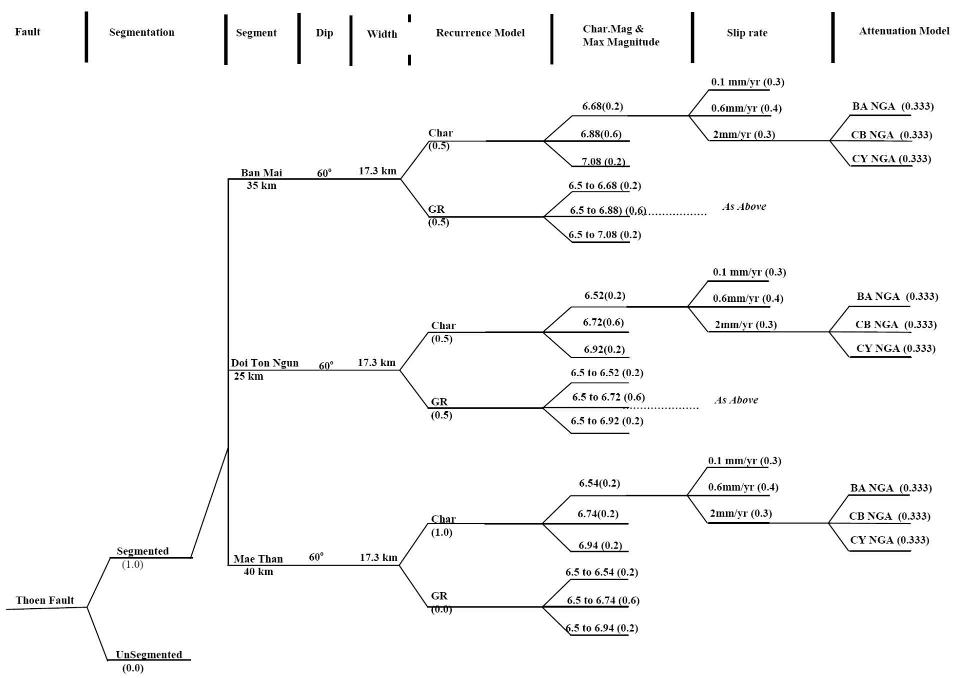

Figure 28: Logic tree diagram of Thoen fault

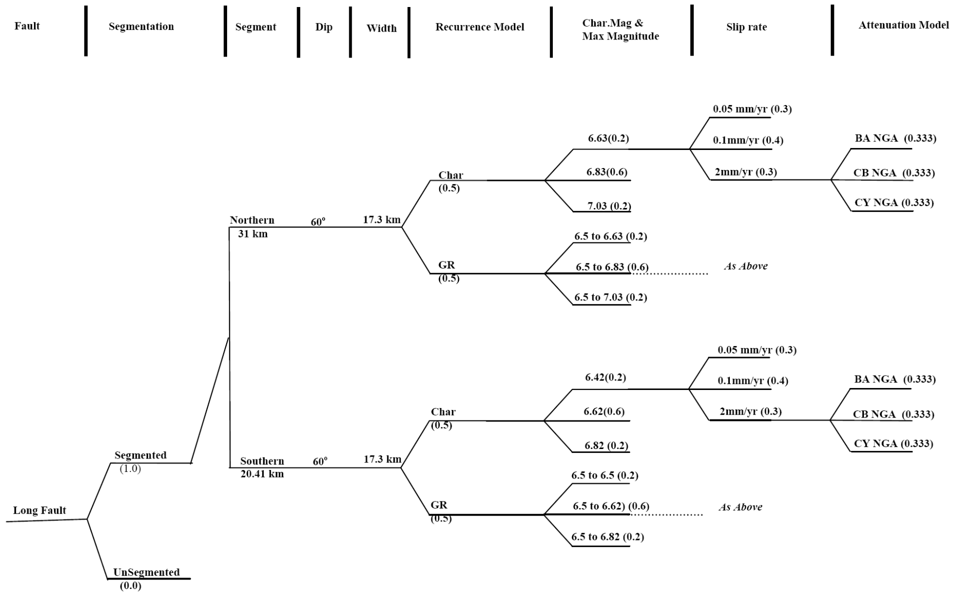

Figure 29: Logic tree diagram of Long fault

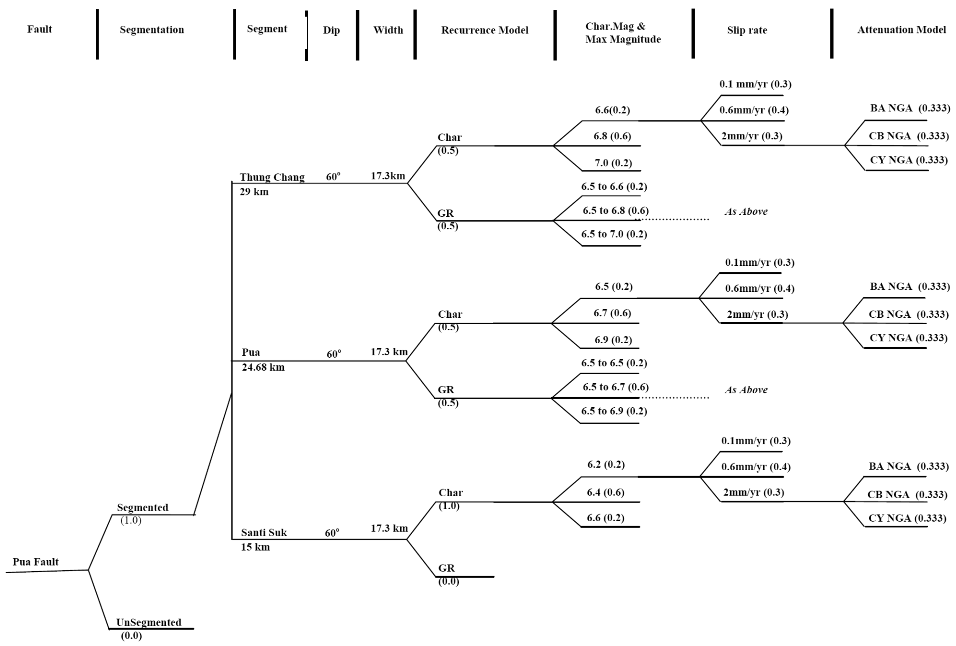

Figure 30: Logic tree diagram of Pua fault

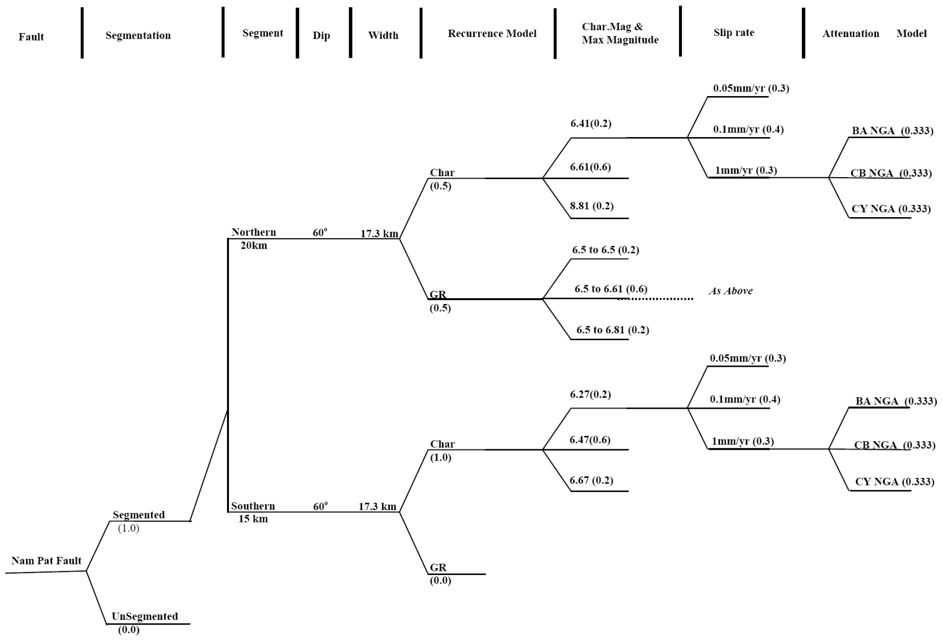

Figure 31: Logic tree diagram of Nam Pat fault

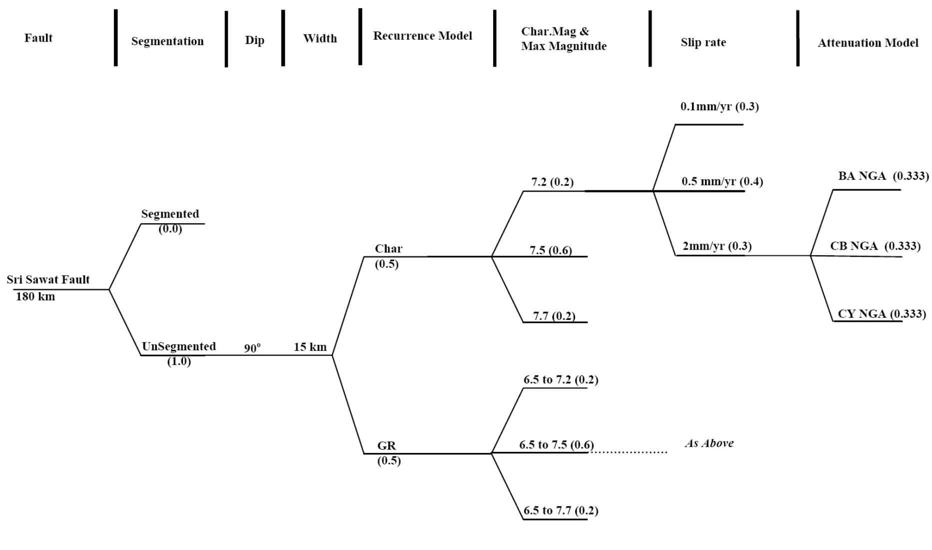

Figure 32: Logic tree diagram of Sri Sawat fault

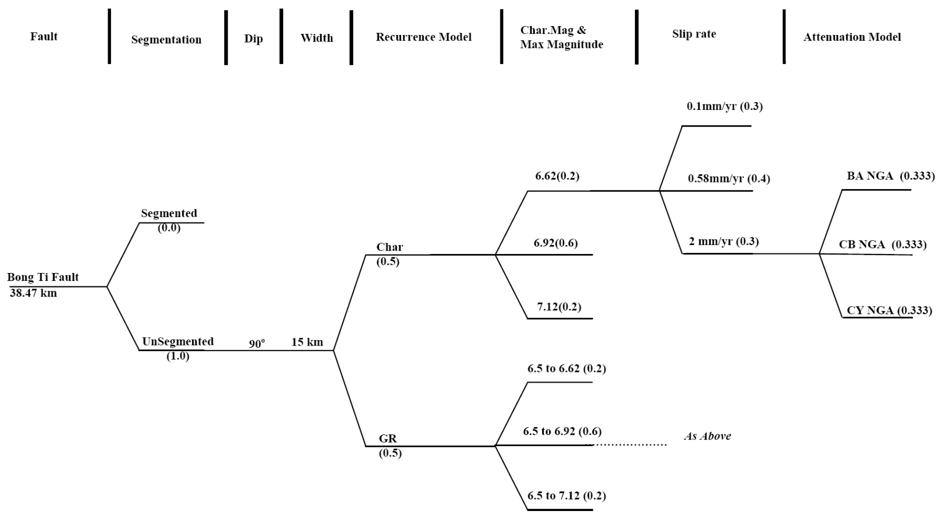

Figure 33: Logic tree diagram of Bong Ti fault

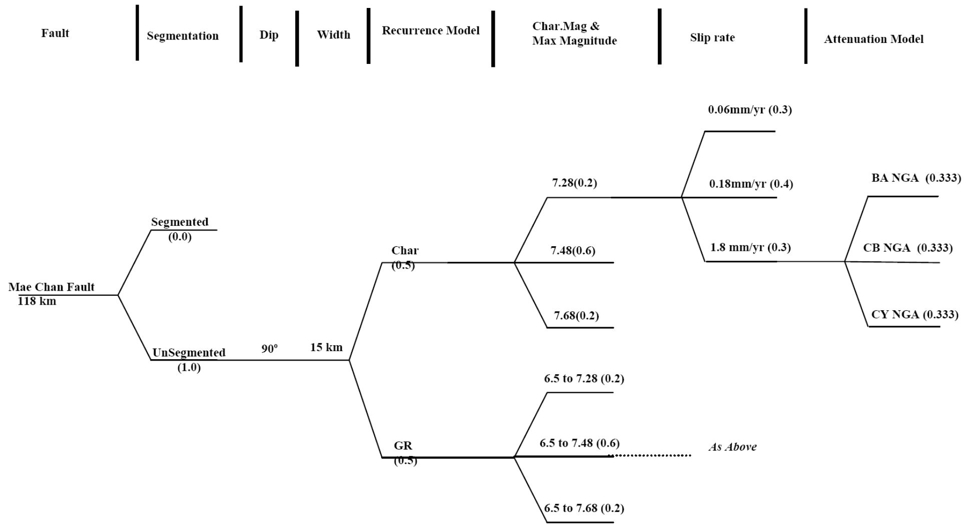

Figure 34: Logic tree diagram of Mae Chan fault

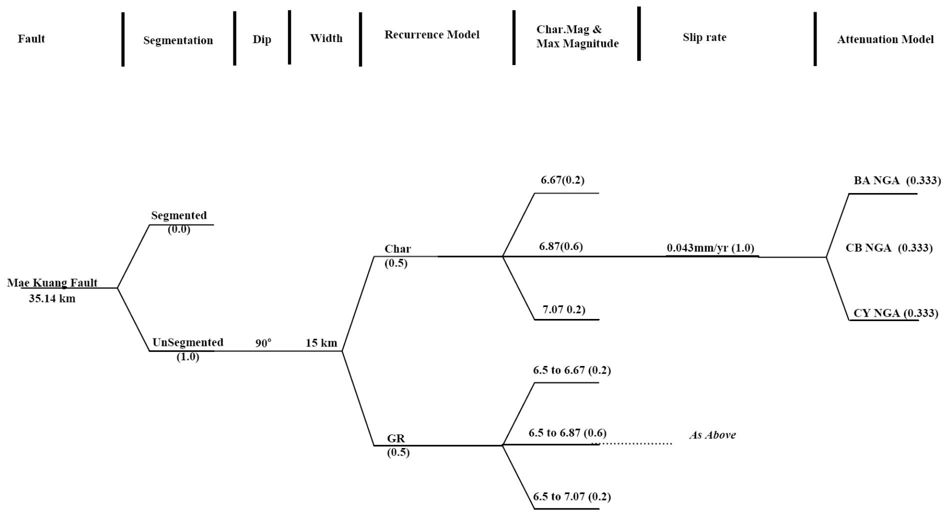

Figure 35: Logic tree diagram of Mae Kuang fault

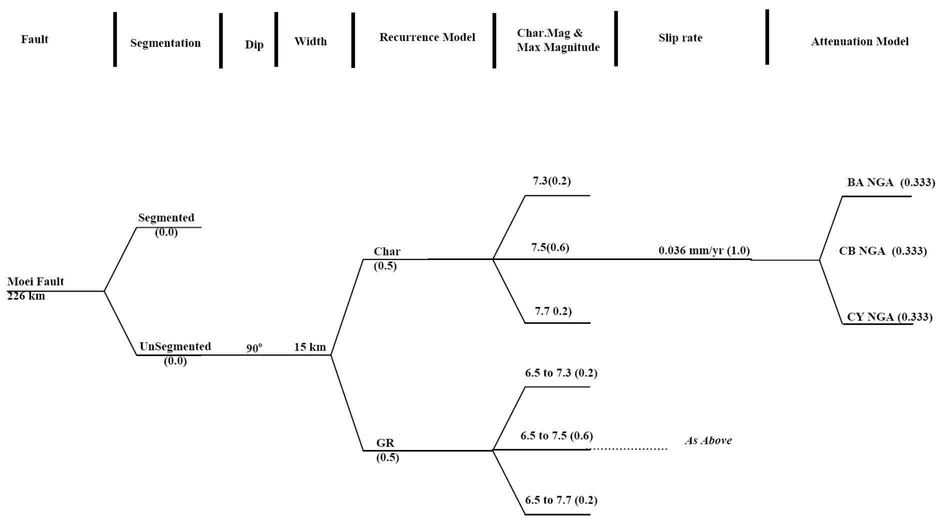

Figure 36: Logic tree diagram of Moei fault

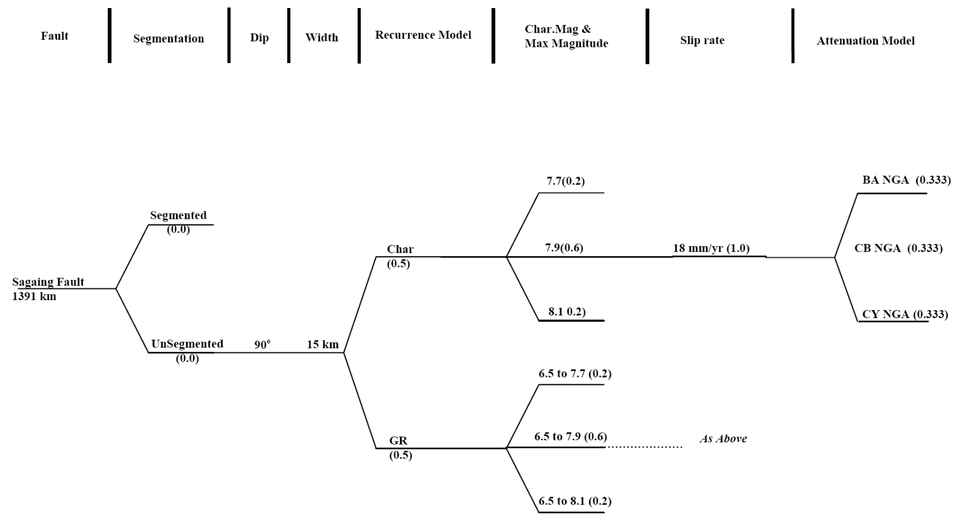

Figure 37:Logic tree diagram of Sagaing fault

The information about crustal faults in and near Thailand are mainly obtained from recent paleoseismic investigations carried out by Woodward-Clyde Federal Services in Northern (DMR, 1996), Western (EGAT, 1998), and Southern Thailand (RID, 2005). The investigations were carried out using an appropriate mix of remote sensing imagery, aerial photographic interpretation, and field investigation. The investigation concentrated on the geomorphic expression of faulting, and the comparison of these features with the features observed along other active faults around the world.

The Sagaing fault in Myanmar is a major right-lateral strike-slip fault in the study region. The high assigned slip rate of 18 mm/yr is based on high rates of strain accumulation suggested by GPS studies (Socquet et al. 2006 and USGS 2007).

The occurrence rate of large magnitude earthquakes on crustal faults is determined from long-term slip rates and characteristic earthquake magnitude (M_C). M_C is estimated from expected rupture length, which may be limited by fault segmentation, by using the relation proposed by Wells and Coppersmith (1994).

Two different approaches are employed to model the magnitude-dependent characteristic of seismicity rate of these crustal faults: GR model and Characteristic Earthquake (CE) model.

In GR model, a GR magnitude-frequency distribution is assumed from the minimum magnitude of 6.5 to the upperbound magnitude (M_{max}). To account for the uncertainty in estimating M_{max}, we consider three different cases with M_{max} set equal to M_C-0.2, M_C, and M_C+0.2. The probabilistic weights of 0.2, 0.6, and 0.2 are assigned to these cases, respectively. In each case, the b-value is set equal to the regional b-value of 0.90, and the a-value is determined from the seismic moment rate, which is computed from the fault slip rate.

In CE model, three characteristic earthquake magnitudes are also considered: M_C-0.2, M_C, and M_C+0.2. The probabilistic weights of 0.2, 0.6, and 0.2 are assigned to these cases, respectively. In each case, the earthquake occurrence rate is computed from the characteristic magnitude and the fault slip rate (to match with the seismic moment rate of the fault), and the magnitude is assumed to be normally distributed around the characteristic value with a standard deviation of 0.12.

4. ATTENUATION MODELS

The ground motion parameters such as PGA and SA at a given site can be estimated from the earthquake magnitude, source-to-site distance, and local site condition by using attenuation models. Traditionally an attenuation model for a specific region is empirically developed from statistical regression analyses of hundreds of earthquake ground motion records. For this region, however, a very limited number of strong motion records are available. One solution to this data limitation is to assume that some existing attenuation models developed for other regions with similar seismotectonic characteristics can adequately represent ground motion attenuation in this region.

In this study, three NGA (Next Generation Attenuation of Ground Motions) attenuation models developed for shallow crustal earthquakes in Western United States and similar active tectonic regions are applied for background earthquakes in BG-I and BG-II and for earthquakes from crustal faults in the study region. These NGA models are developed by Boore and Atkinson (2007), Campbell and Bozorgnia (2007), and Chiou and Youngs (2007) under the Next Generation Attenuation Relation project. We assign equal probablilistic weight to each of these three models in the logic trees analysis.

For subduction zone earthquakes in SD-A, SD-B and SD-C, we adopt three subduction zone attenuation models developed by Youngs et al. (1997), Atkinson and Boore (2003, global model), and Zhao et al. (1997). Probabilistic weights assigned to these models are 0.25, 0.25, and 0.50, respectively.

The above selected sets of attenuation models as well as their corresponding probabilistic weights are identical to those used by USGS in their recent seismic hazard study of Southeast Asia in 2007 (USGS, 2007). These attenuation models are illustrated by Figures 38-60.

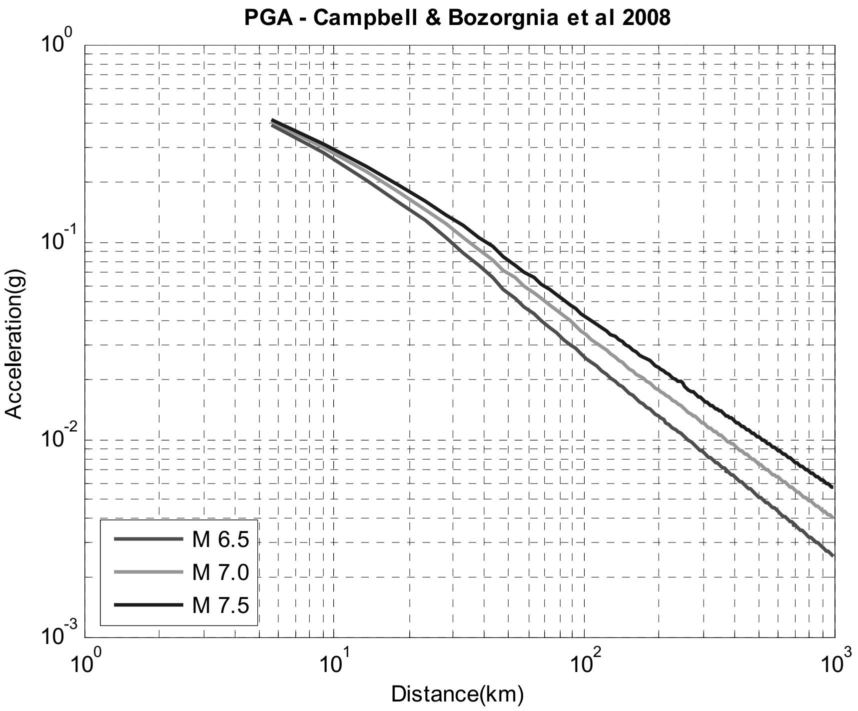

Figure 38: Campbell & Bozorgnia (2008) NGA attenuation relation for peak ground acceleration

Figure 39:Campbell & Bozorgnia (2008) NGA attenuation relation for spectral acceleration at 0.2 sec

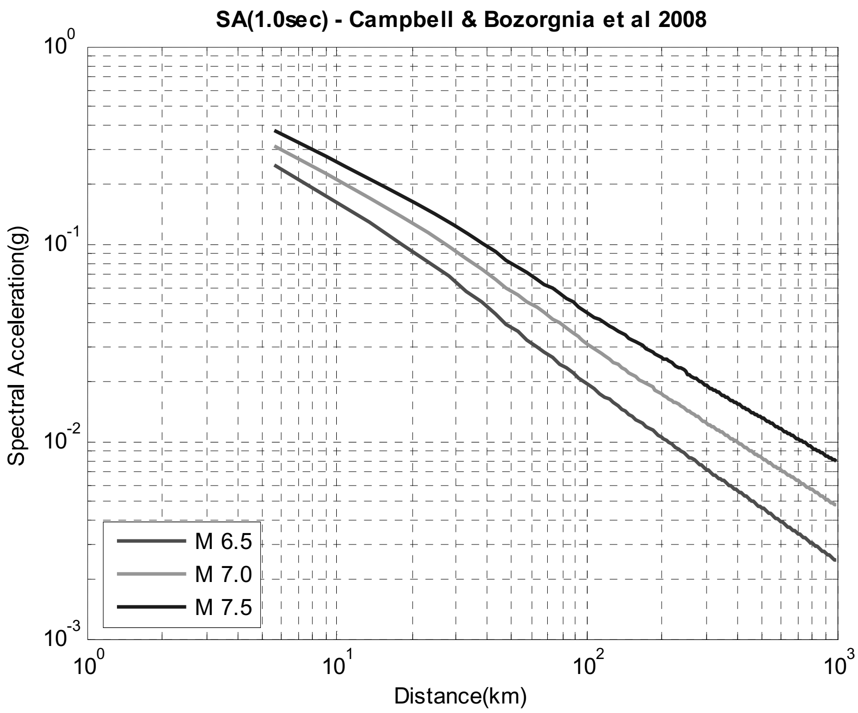

Figure 40: Campbell & Bozorgnia (2008) NGA attenuation relation for spectral acceleration at 1.0 sec

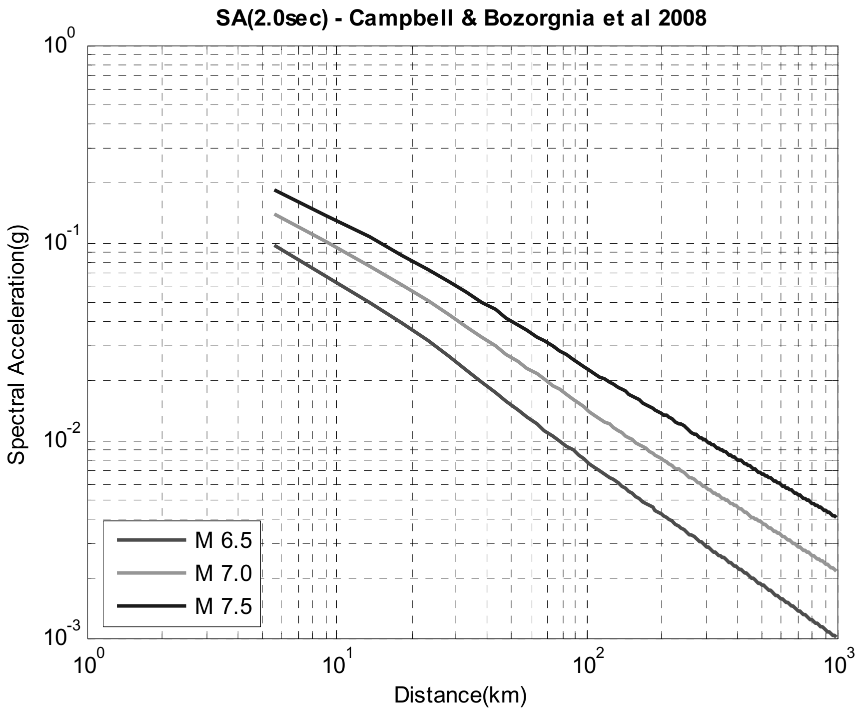

Figure 41: Campbell & Bozorgnia (2008) NGA attenuation relation for spectral acceleration at 2.0 sec

Figure 42: Boore & Atkinson (2008) NGA attenuation relation for peak ground acceleration

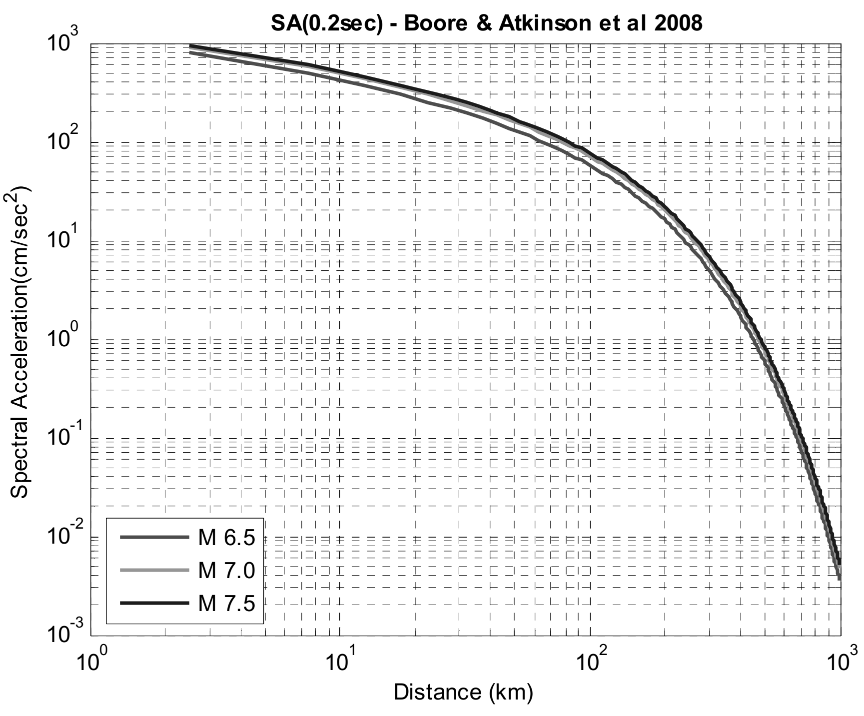

Figure 43:Boore & Atkinson (2008) NGA attenuation relation for spectral acceleration at 0.2 sec

Figure 44: Boore & Atkinson (2008) NGA attenuation relation for spectral acceleration at 1.0 sec

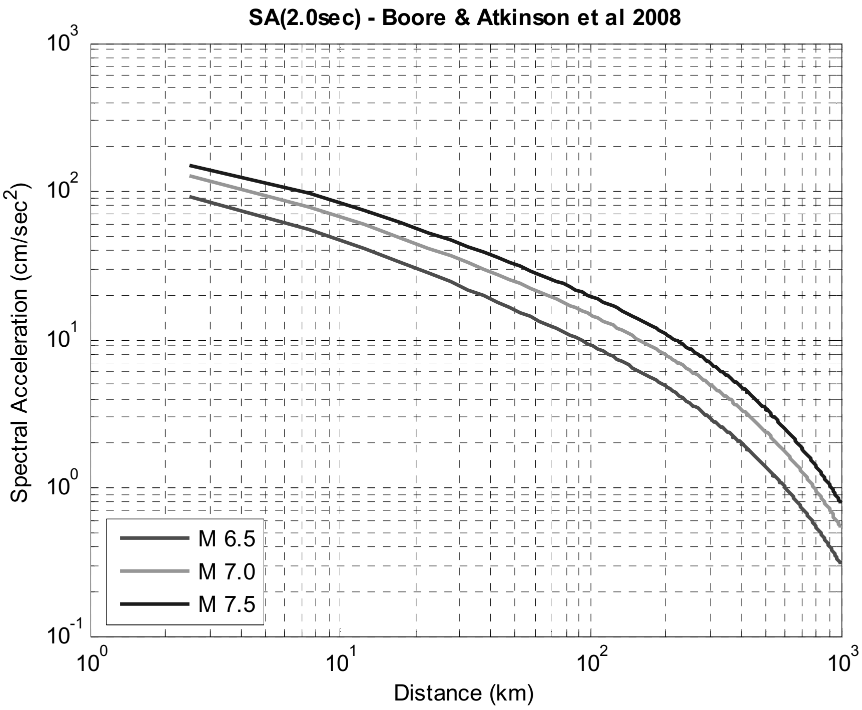

Figure 45: Boore & Atkinson (2008) NGA attenuation relation for spectral acceleration at 2.0 sec

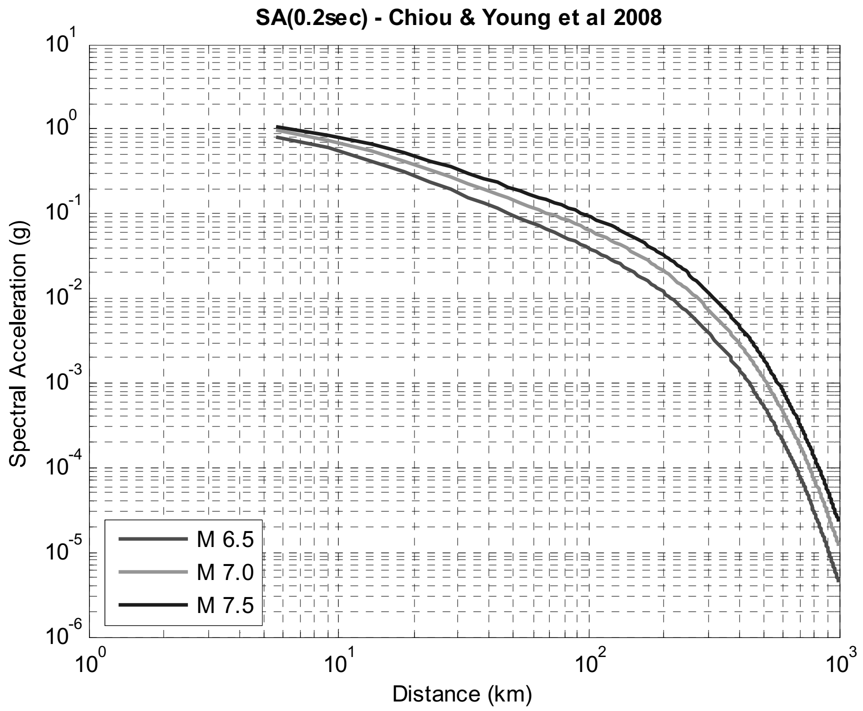

Figure 46: Chiou & Youngs (2008) NGA attenuation relation for spectral acceleration at 0.2 sec

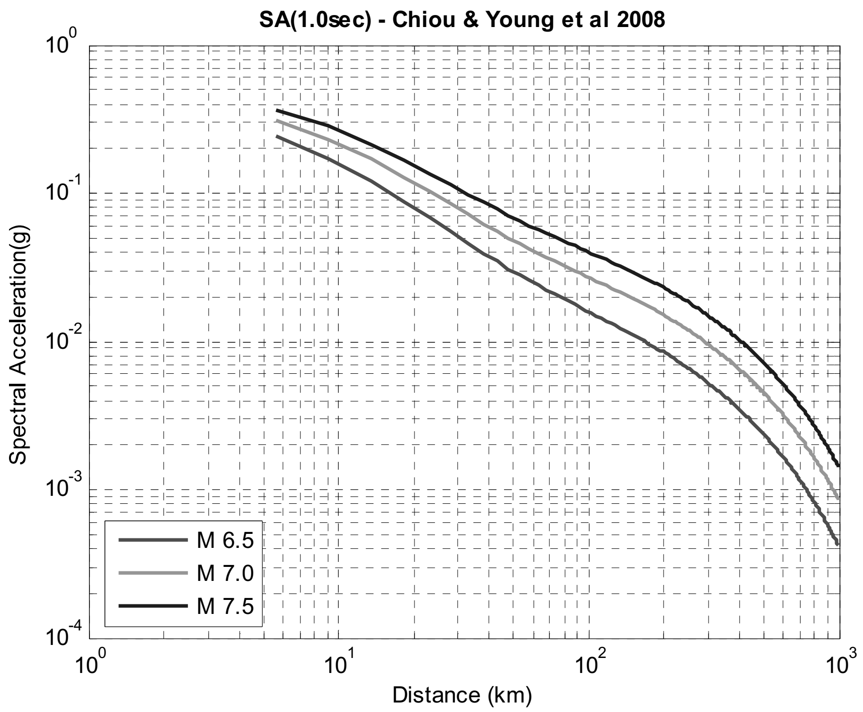

Figure 47: Chiou & Youngs (2008) NGA attenuation relation for spectral acceleration at 1.0 sec

Figure 48: Chiou & Youngs (2008) NGA attenuation relation for spectral acceleration at 2.0 sec

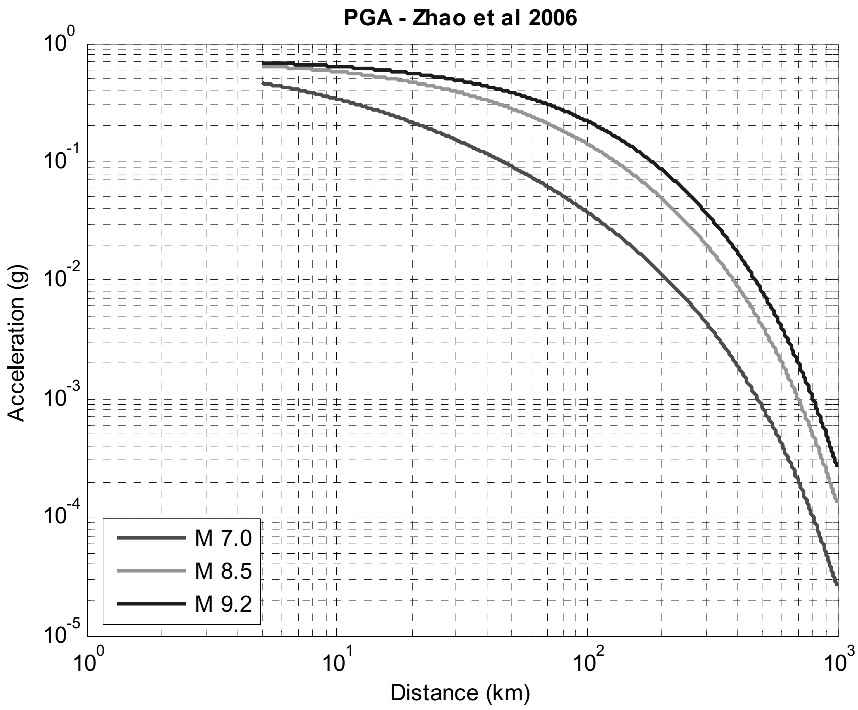

Figure 49: Zhao (2006) Subduction attenuation relation for peak ground acceleration

Figure 50: Zhao (2006) Subduction attenuation relation for spectral acceleration at 0.2 sec

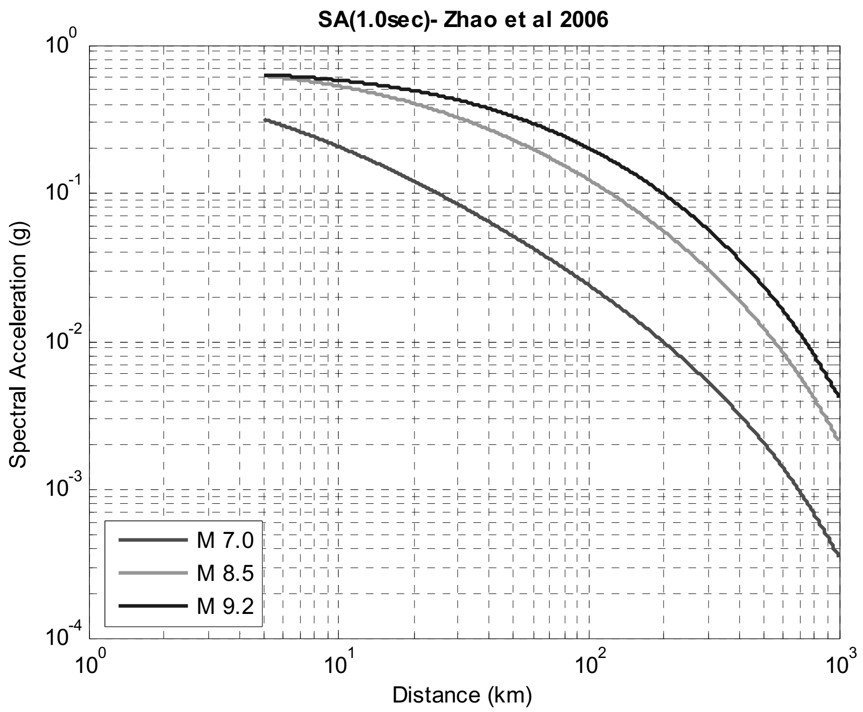

Figure 51: Zhao (2006) Subduction attenuation relation for spectral acceleration at 1.0 sec

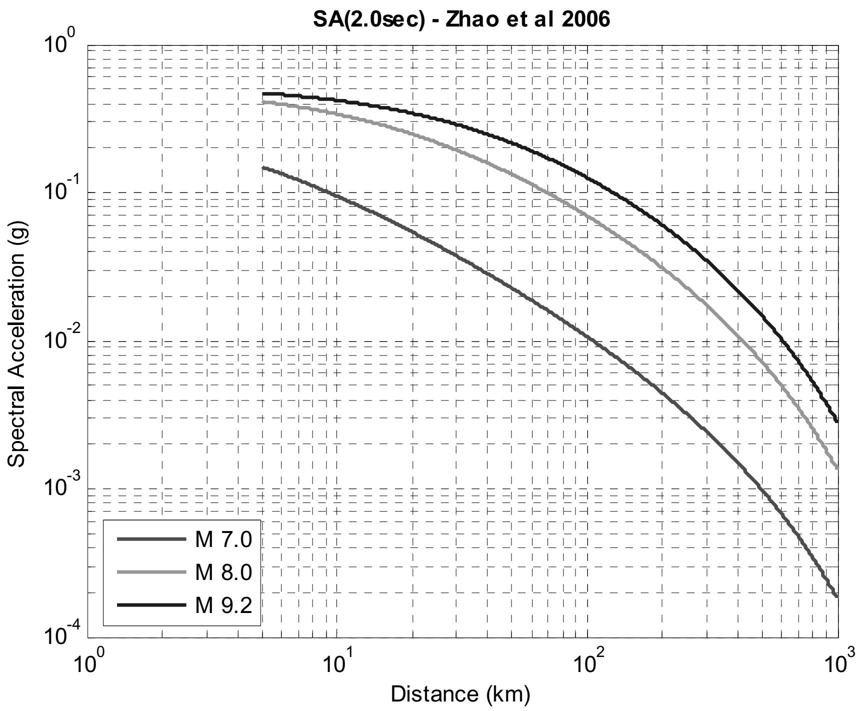

Figure 52: Zhao (2006) Subduction attenuation relation for spectral acceleration at 2.0 sec

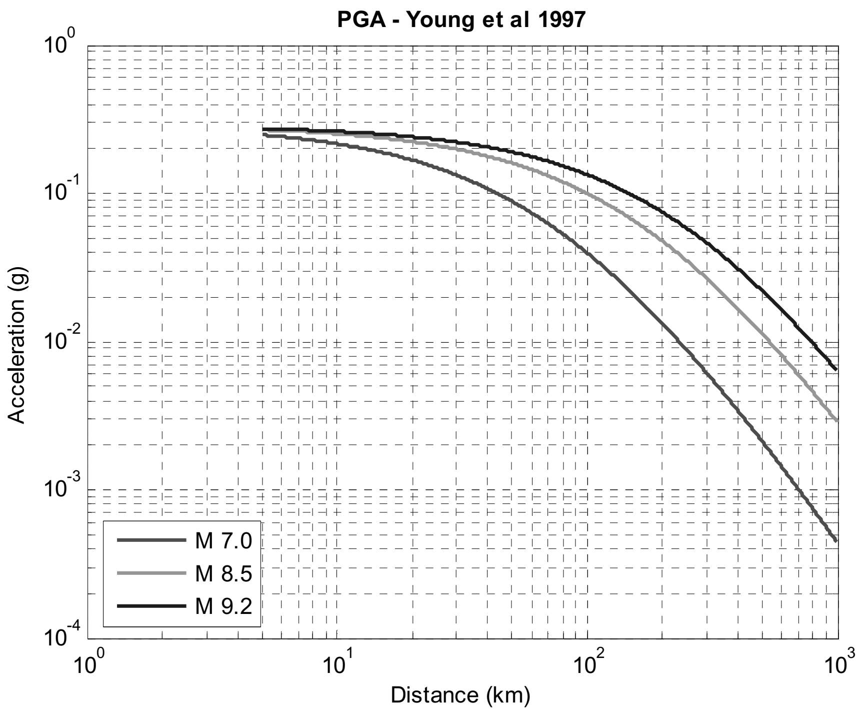

Figure 53: Young (1997) Subduction attenuation relation for peak ground acceleration

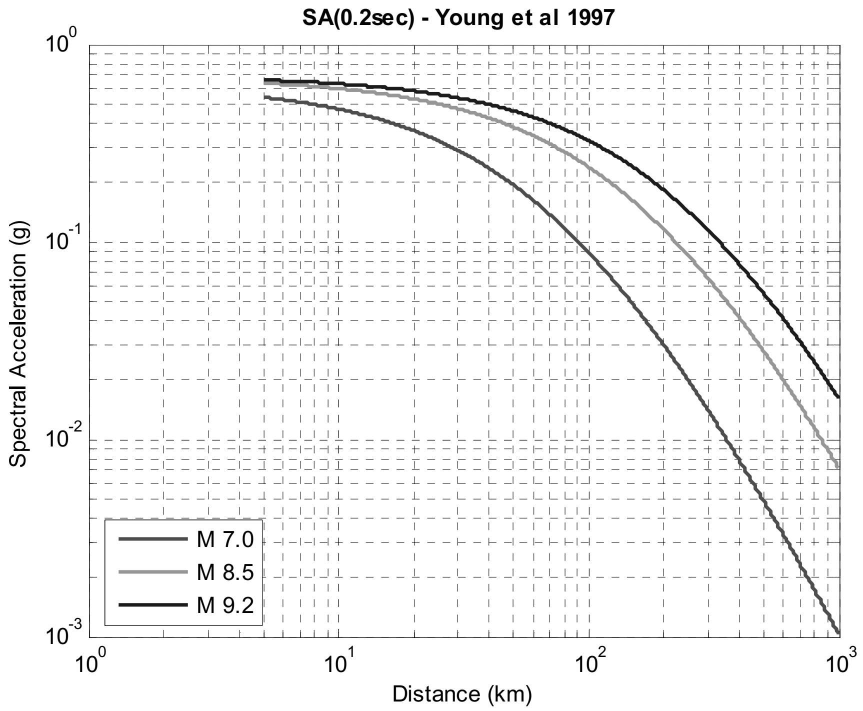

Figure 54: Young (1997) Subduction attenuation relation for spectral acceleration at 0.2 sec

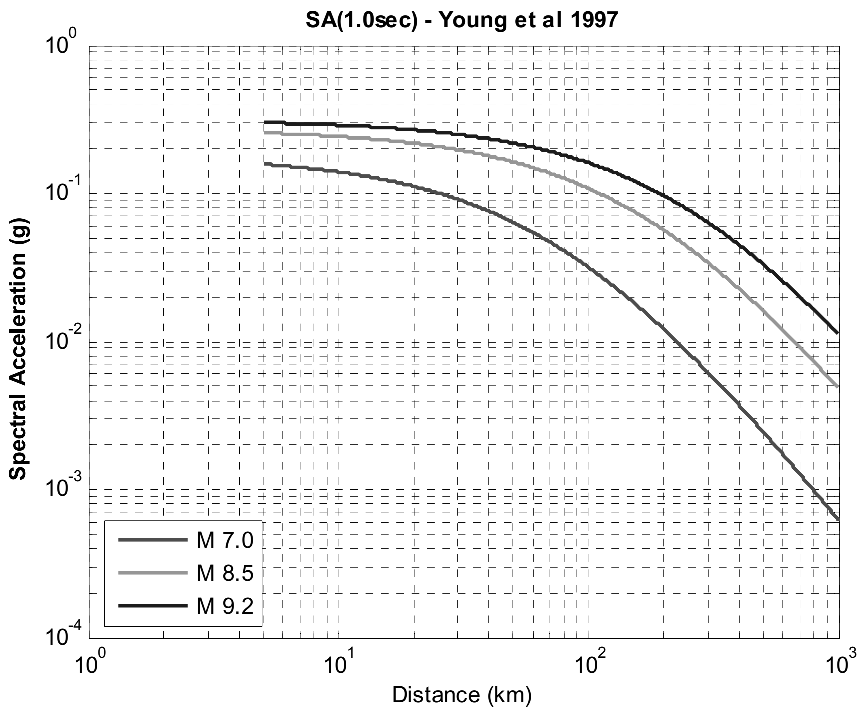

Figure 55: Young (1997) Subduction attenuation relation for spectral acceleration at 1.0 sec

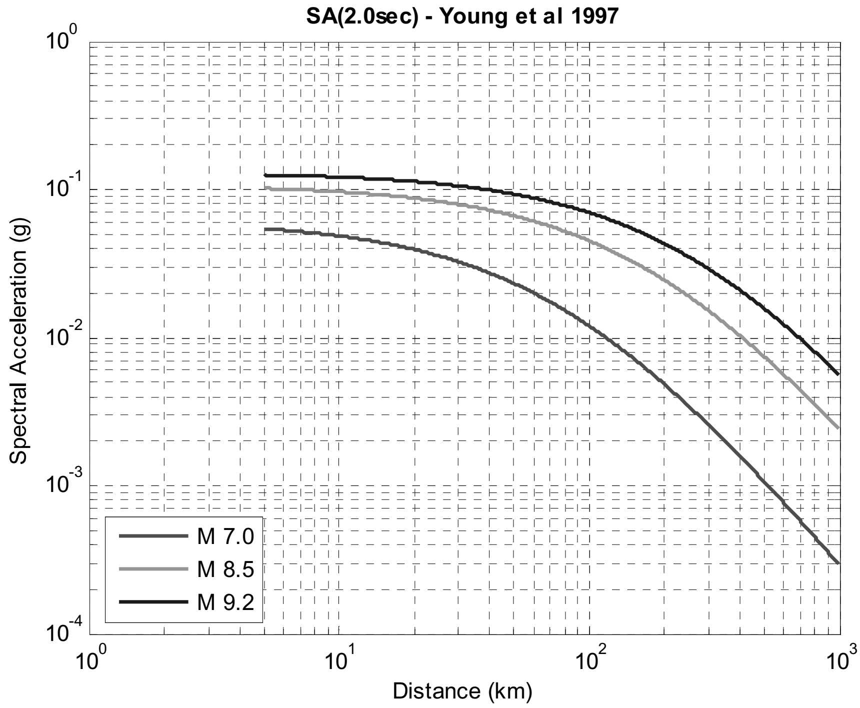

Figure 56: Young (1997) Subduction attenuation relation for spectral acceleration at 2.0 sec

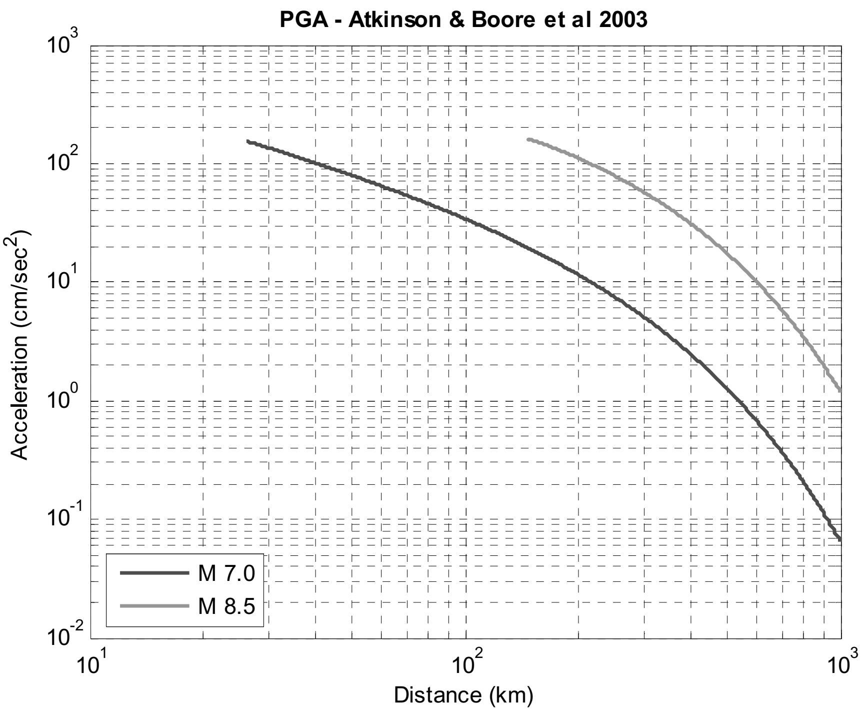

Figure 57: Atkinson & Boore (2003) Subduction attenuation relation for peak ground acceleration

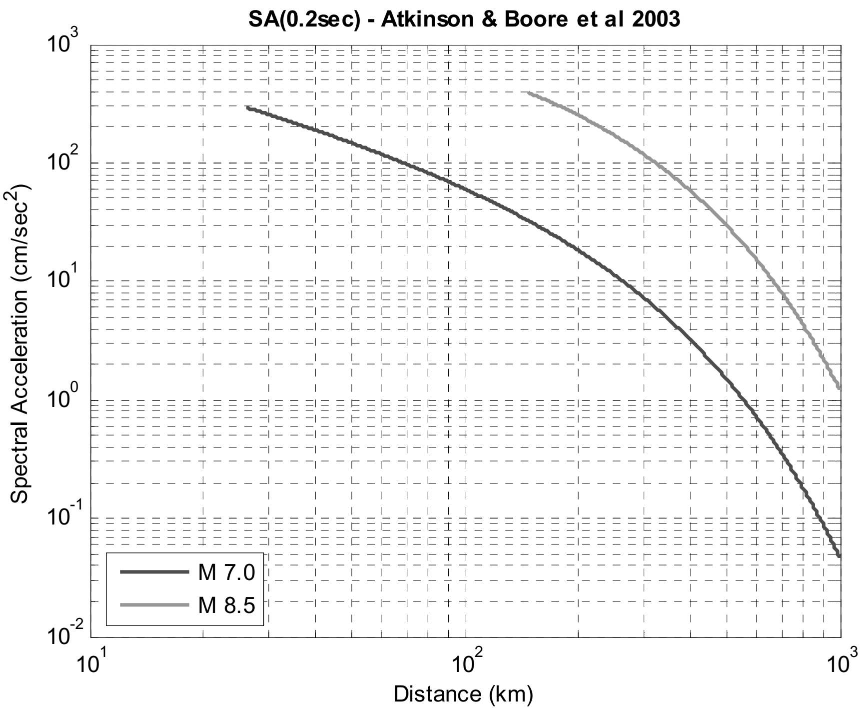

Figure 58: Atkinson & Boore (2003) Subduction attenuation relation for spectral acceleration at 0.2 sec

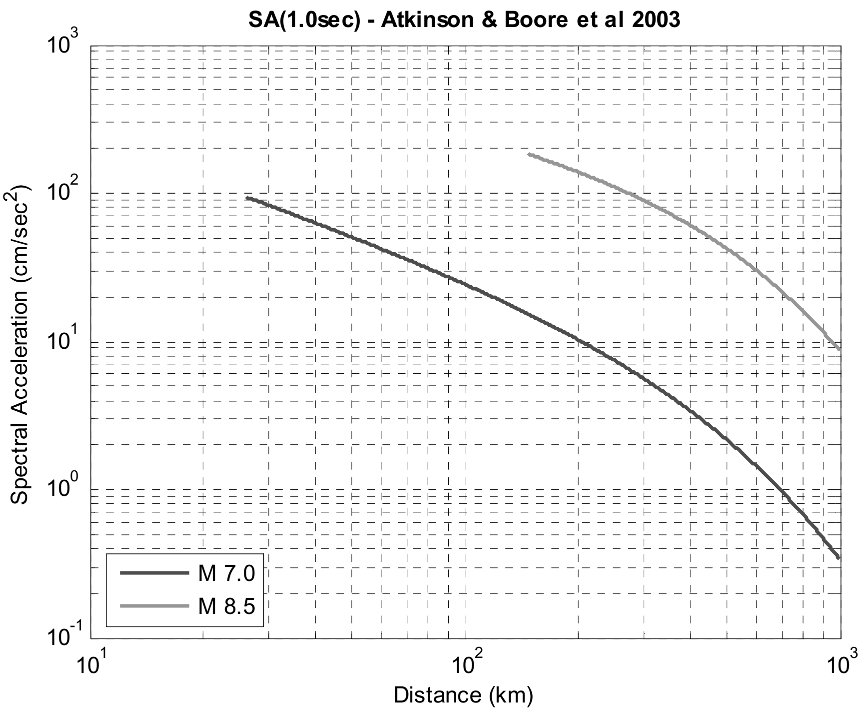

Figure 59: Atkinson & Boore (2003) Subduction attenuation relation for spectral acceleration at 1.0 sec

Figure 60: Atkinson & Boore (2003) Subduction attenuation relation for spectral acceleration at 2.0 sec

5. PROBABILISTIC SEISMIC HAZARD ANALYSIS

The probabilistic seismic hazard analysis (PSHA) is carried using the USGS software for PSHA (Harmsen, 2007). This is an open-source software in Fortran-95 code developed and used by the USGS for making and updating the US National Seismic Hazard map.

5.1 Results

5.1.1 Seismic Hazard Maps

The PSHA results are presented by several seismic hazard maps:

- map of peak ground acceleration with a 10-percent probability of exceedance in a 50-year exposure period (Figure 17)
- map of peak ground acceleration with a 2-percent probability of exceedance in a 50-year exposure period (Figure 18)
- map of spectral acceleration at 0.2 sec with a 2-percent probability of exceedance in a 50-year exposure period (Figure 19)
- map of spectral acceleration at 1.0 sec with a 2-percent probability of exceedance in a 50-year exposure period (Figure 20)
- map of spectral acceleration at 2.0 sec with a 2-percent probability of exceedance in a 50-year exposure period (Figure 21)

All these seismic hazard maps are made using a reference site condition that is specified to be the boundary between NEHRP (National Earthquake Hazards Reduction Program) classes B and C (rock site), with an average shear-wave velocity in the upper 30 m of the crust of 760 m/s.

The PGA map for 10 percent probability of exceedance (10% P_e), which corresponds to a return period of 475 years, shows a pattern of seismic hazard that is well correlated with the seismicity rate 10^a (see Figure 8). The effect of low-slip-rate crustal faults in Thailand on seismic hazard is not so clear on this map. On the other hand, the effect of crustal faults becomes evidence in the PGA map (as well as spectral acceleration maps) for 2% P_e, which corresponds to a return period of 2475 years. The map clearly shows locally high seismic hazard levels at the locations of some crustal faults. The results confirm the important of crustal fault sources on the seismic hazard of Thailand.

The computed probabilistic ground motion parameters at some selected locations in Thailand are compared with those obtained from other earlier seismic hazard studies in Table 5.

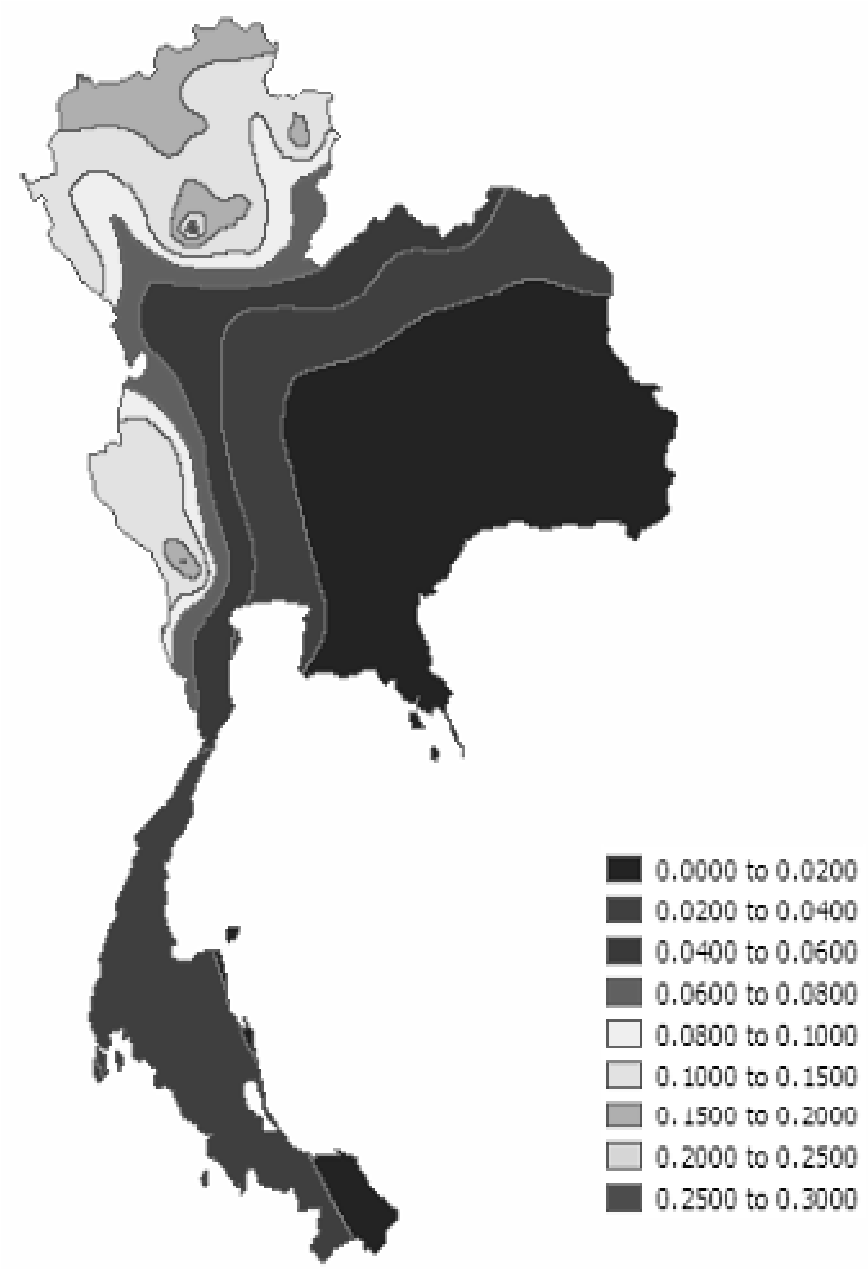

Figure 61: Map of peak ground acceleration with a 10-percent probability of exceedance in a 50-year exposure period (unit: g)

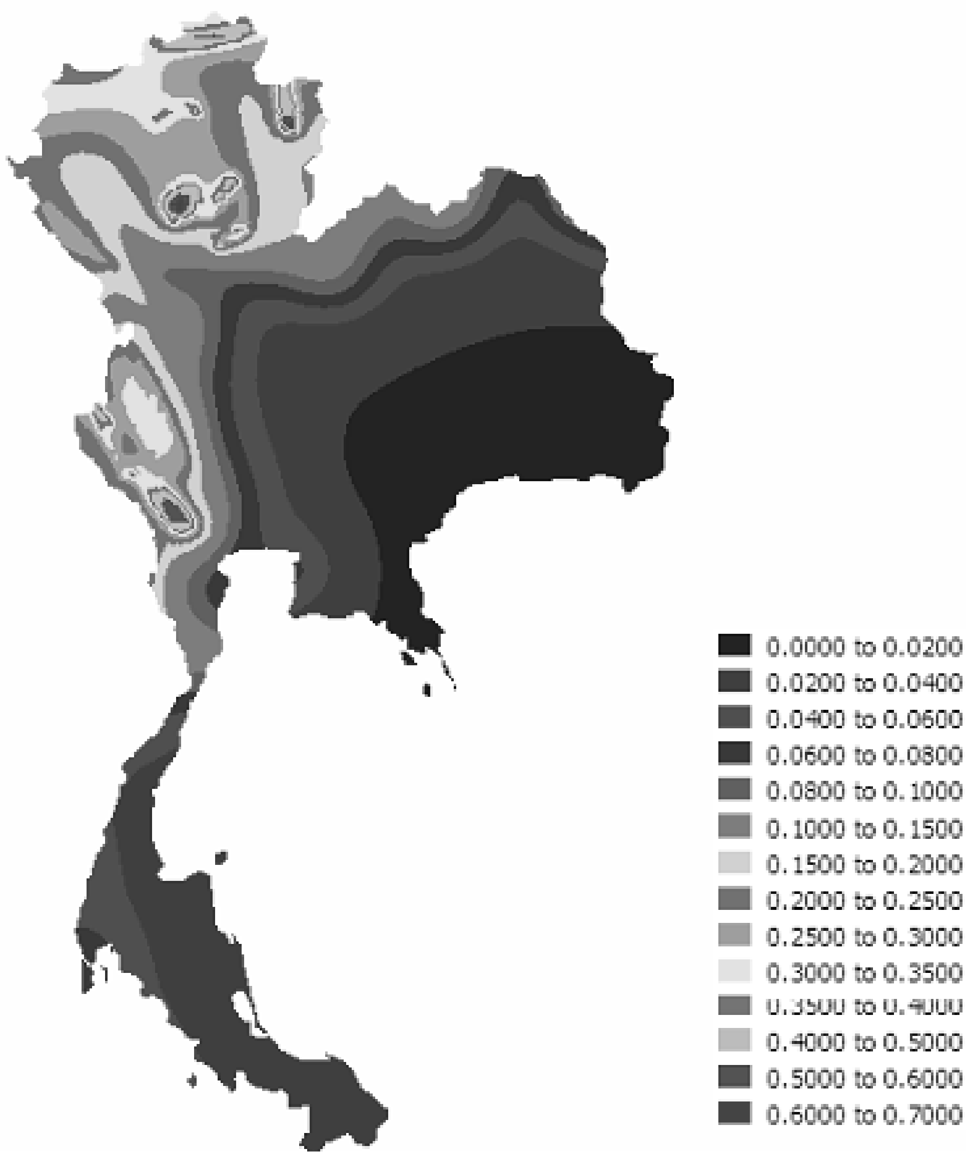

Figure 62: Map of peak ground acceleration with a 2-percent probability of exceedance in a 50-year exposure period (unit: g)

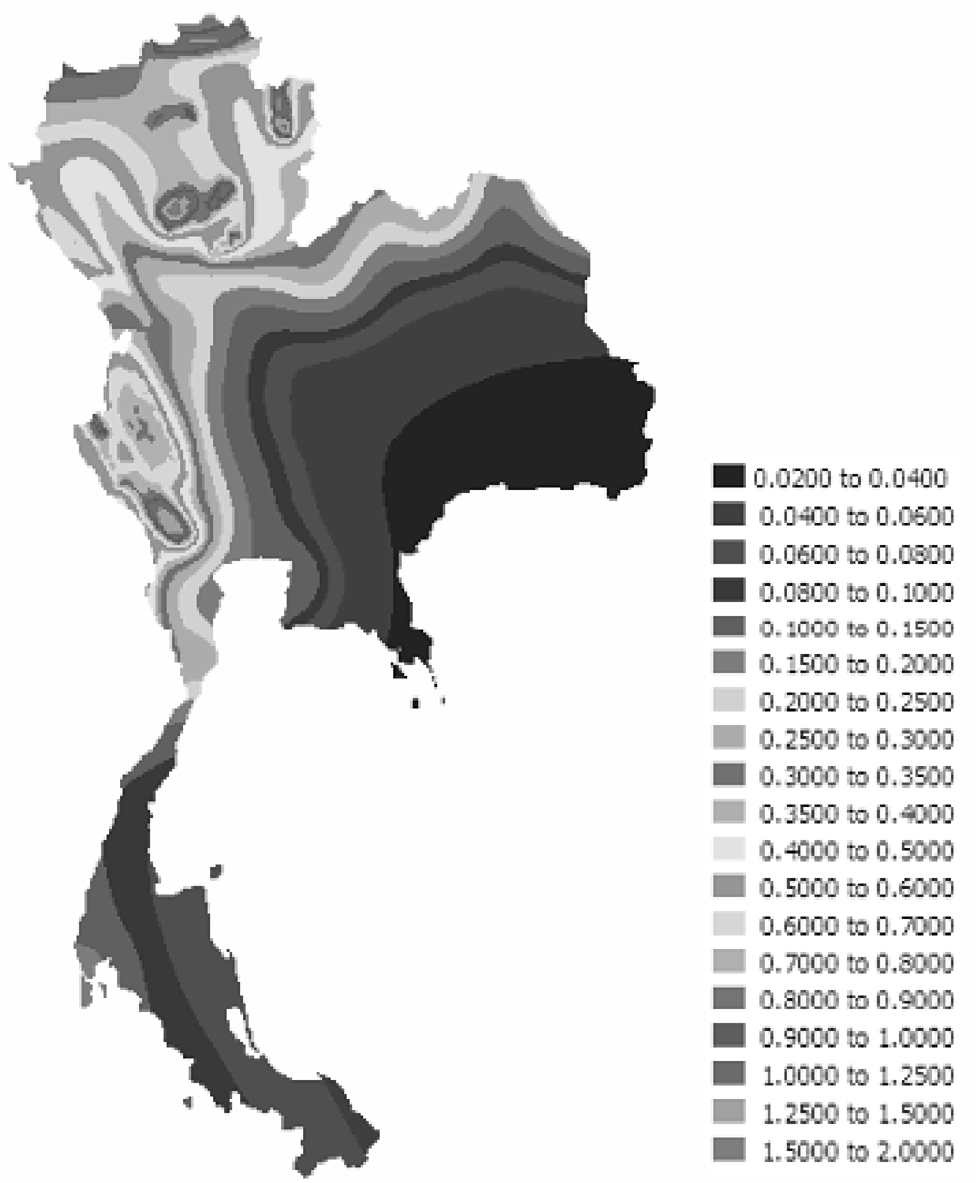

Figure 63: Map of spectral acceleration at 0.2 sec with a 2-percent probability of exceedance in a 50-year exposure period (unit: g)

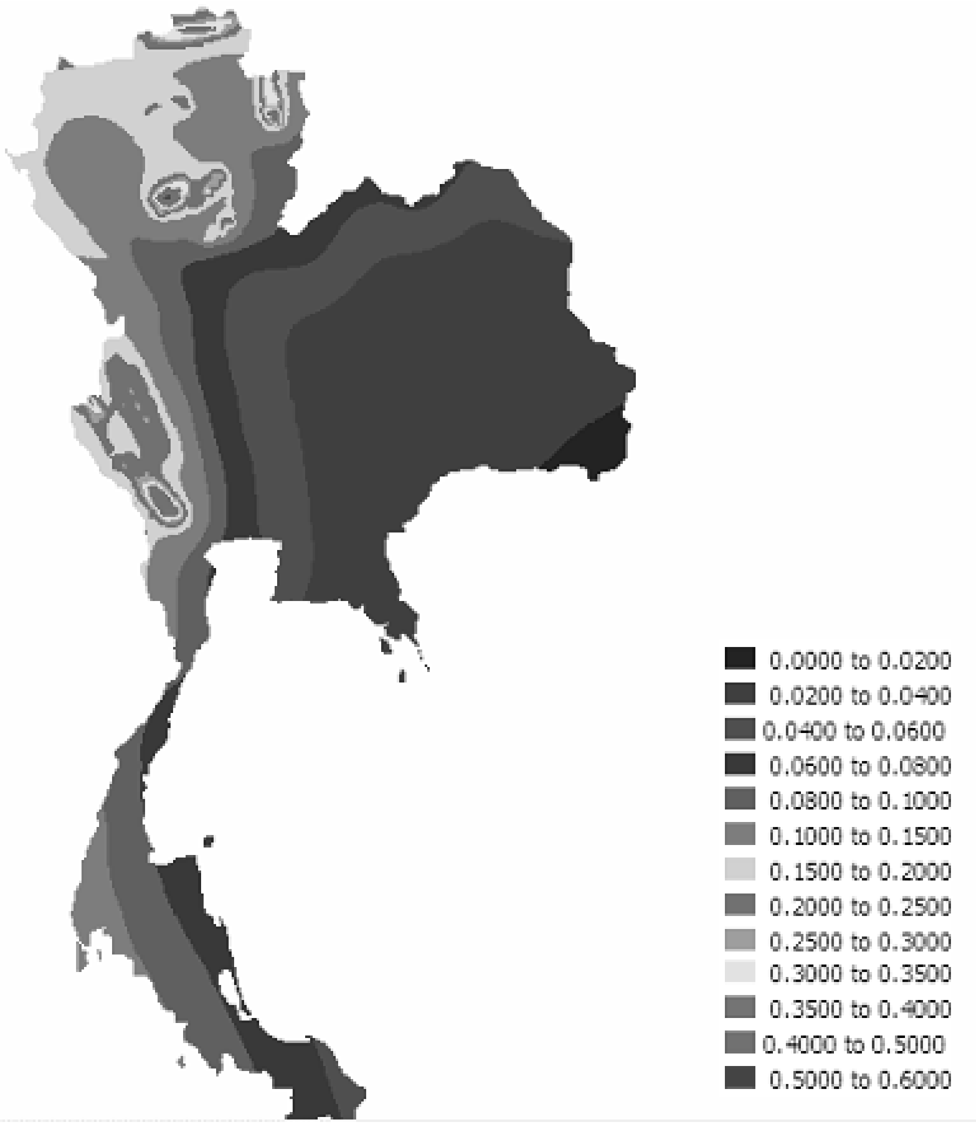

Figure 64: Map of spectral acceleration at 1.0 sec with a 2-percent probability of exceedance in a 50-year exposure period (unit: g)

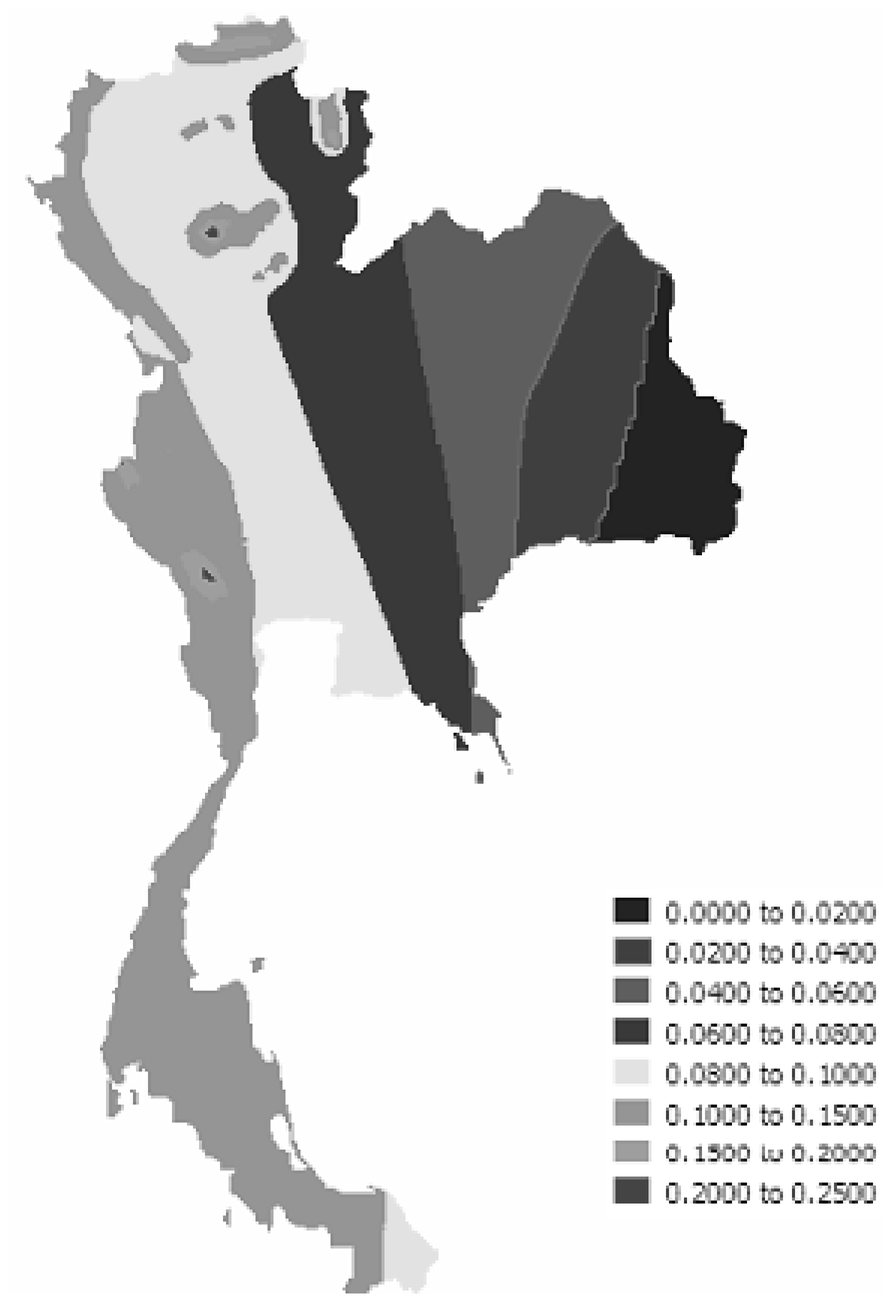

Figure 65: Map of spectral acceleration at 2.0 sec with a 2-percent probability of exceedance in a 50-year exposure period (unit: g)

Table 5: Comparison of probabilistic ground motion parameters from the current study with those obtained from other seismic hazard studies

Location	PGA (AIT)	PGA (USGS)	PGA (WC)	SA(1.0s) (AIT)	SA(1.0s) (CHULA)	SA(1.0s) (USGS)	SA(0.2s) (AIT)	SA(0.2s) (CHULA)	SA(0.2s) (USGS)	SA(2.0s) (AIT)
Silom, BKK	*0.060*			*0.067*			*0.1449*			*0.092*
BKK	*0.066*	*0.10*		*0.0718*	*0.04-0.06*	*0.07*	*0.1588*	*0.2*	*0.15*	*0.093*
Kanchanaburi	*0.3422*	*0.15*		*0.2486*	*0.15*	*0.12*	*0.8253*	*0.6*	*0.5*	*0.149*
Chiang Mai	*0.2879*	*0.12*		*0.1552*	*0.3*	*0.1*	*0.7091*	*0.8*	*0.30*	*0.092*
Kao Laem Dam	*0.3311*	*0. 20-0.25*	*0.49*	*0.2407*	*0.15*	*0.15-0.20*	*0.7899*	*0.6*	*0.5-0.6*	*0.145*
Srinakarin Dam	*0.318*	*0.15-0.20*	*0.55*	*0.2371*	*0.15*	*0.15-0.20*	*0.7747*	*0.6*	*0.5-0.6*	*0.142*
Kaeng Sue Ten	*0.2173*	*0.25*		*0.1208*	*0.15-0.20*	*0.20*	*0.5467*	*0.6-0.7*	*0.5-0.6*	*0.078*

AIT: *Current study—spatially smoothed grid seismicity and active faults + 3 NGA attenuation models (Chiou-Youngs 2007, Campbell-Bozorgnia 2007, Boore-Atkinson 2007).*
CHULA: *Dr. Anat's work—seismic area sources with no explicit active faults + WNA attenuation model (?)*
USGS: *USGS's recent seismic hazard assessment study for Southeast Asia (2007)*
WC: *Woodward Clyde's study*

5.1.2 Seismic Hazard in Bangkok

The seismic hazard in Bangkok is contributed by earthquakes from many sources near and far. To gain insight into this issue, hazard curves obtained from the analysis of spectral acceleration at four periods of vibration are shown in Figures 62-65. The contributions from different earthquake sources are illustrated by disaggregated hazard curves, where each curve represents the hazard from only one earthquake source. The results show that the seismic hazard at short period (0.2 sec) is contributed mainly by crustal faults and to a lesser extent by background seismicity. The contribution from distant subduction earthquakes is negligibly low. This contribution, however, rapidly increases with the increasing in period, and finally becomes the dominant one for hazard at long periods (2.0 and 3.0 sec).

A uniform hazard spectrum for Bangkok is then constructed from the computed PGA and spectral accelerations for 2% P_e as shown by the violet line in Figure 66. The green, red, and blue lines represent the hazard contributions from subduction zones, crustal faults, and background seismicity, respectively. Although the analysis is made up to the period of 3.0 sec, the hazard spectrum is extended up to the period of 6.0 sec by assuming that the spectral acceleration is inversely proportional to period.

Since the uniform hazard spectrum of violet line is made for the NEHRP site class B/C (rock site), it is then transformed into the UHS (Uniform Hazard spectrum) for soft Bangkok site condition. The transformation is made by multiplying the UHS for site class B/C with the period-dependent spectral amplification ratio in the column "average" in Table 5. The period-dependent spectral amplification ratio is estimated from the transfer functions of Bangkok soil profiles A2 and B1 (see pages 42 and 43 in CPI, 2009) and assumed frequency composition of ground shaking corresponding to the spectral period. The spectral amplification ratios at 0.2 sec and 1.0 sec are similar to those of NEHRP site class E (soft soil site) and those at long periods (2.0-6.0 sec) are similar to those of ARUP's study.

The resulting UHS for soft Bangkok soil is shown by the orange line in Figure 66 and the green line in Figure 67**.**

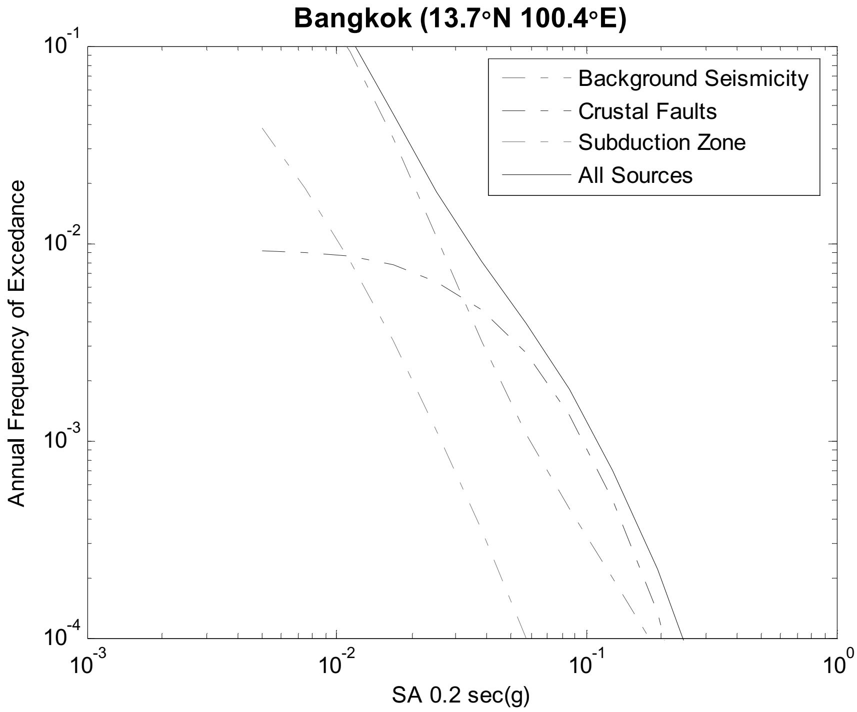

Figure 66: Computed hazard for spectral acceleration at 0.2 sec in Bangkok, and contributions of three different earthquake sources to the hazard

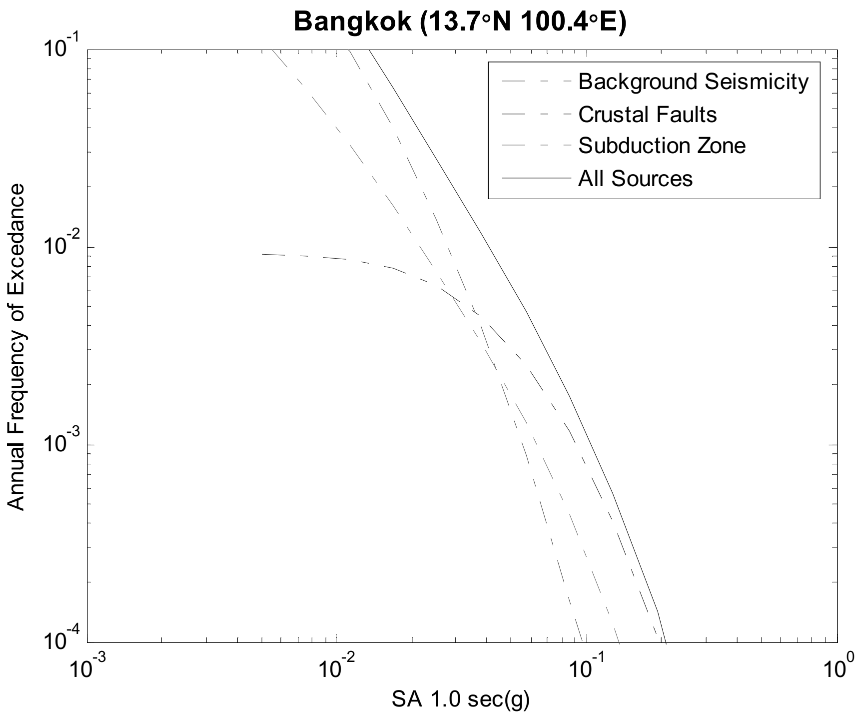

Figure 67: Computed hazard for spectral acceleration at 1.0 sec in Bangkok, and contributions of three different earthquake sources to the hazard

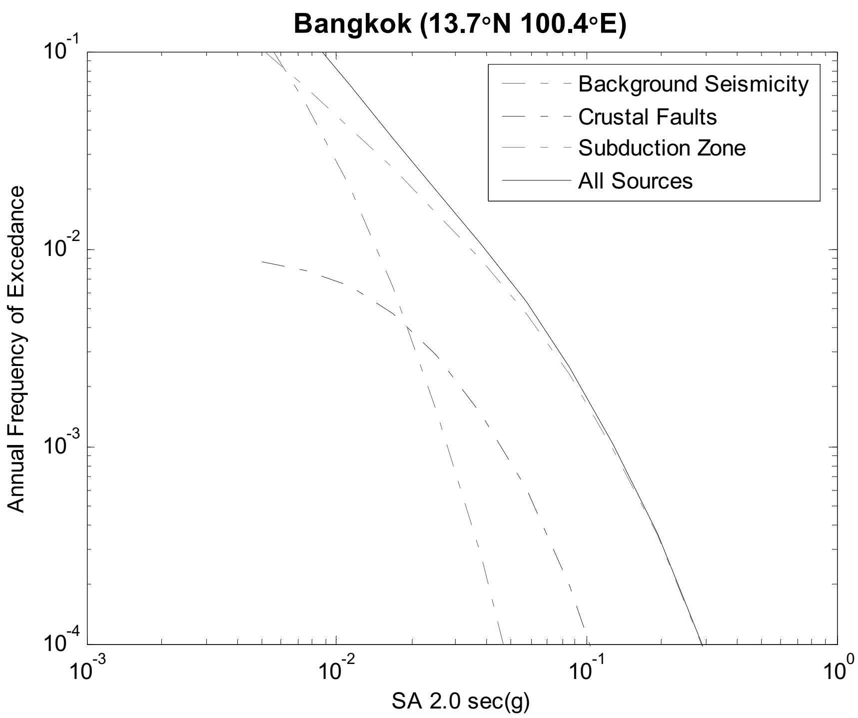

Figure 68: Computed hazard for spectral acceleration at 2.0 sec in Bangkok, and contributions of three different earthquake sources to the hazard

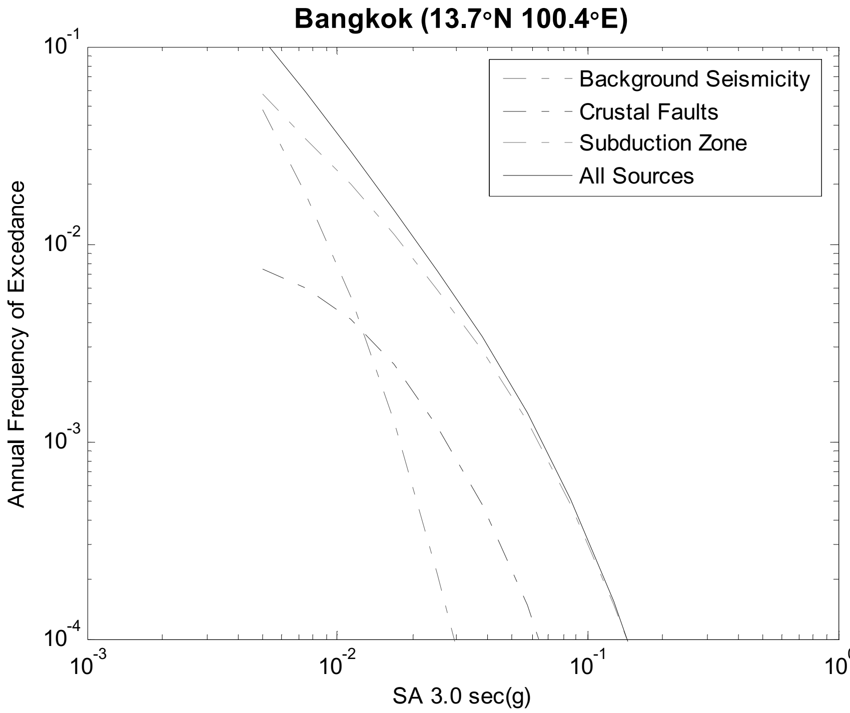

Figure 69: Computed hazard for spectral acceleration at 3.0 sec in Bangkok, and contributions of three different earthquake sources to the hazard

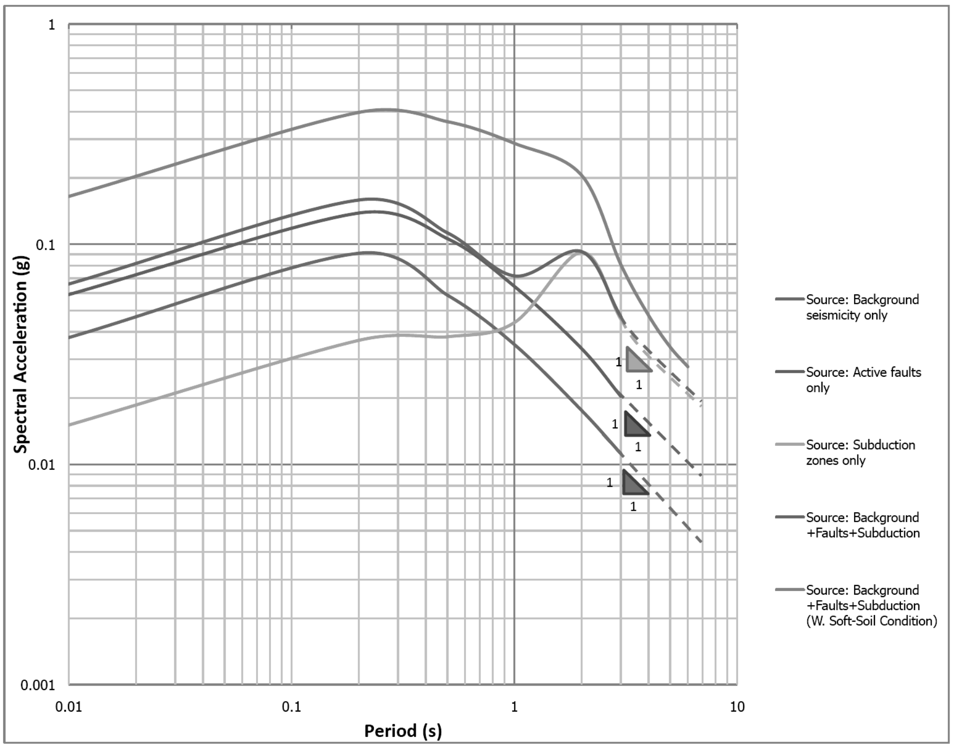

Figure 70: Uniform Hazard Spectrum of Bangkok for 2-percent probability of exceedance, and contributions of three earthquake sources to the pectrum

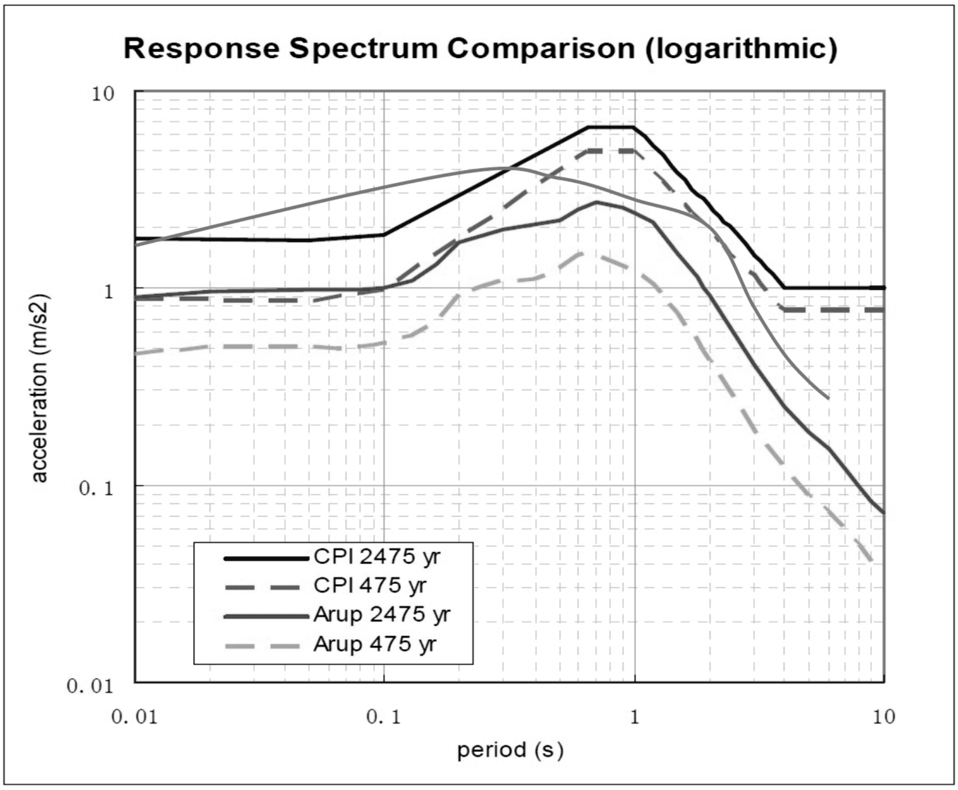

Figure 71: Comparison of uniform hazard spectra

REFERENCES

Atkinson, G.M., and Boore, D.M., (2003), "Empirical ground-motion relations for Subduction-zone earthquakes and their application to Cascadia and other regions", *Bull. Seism. Soc. Am.,* Vol. 93, pp 1703-1729.

Boore, D.M. and Atkinson, G.M. (2008), "Ground-motion prediction equations for the average horizontal component of PGA, PGV, and 5%-damped PSA at spectral periods between 0.01 s and 10.0 s", *Earthquake Spectra*, Vol. 24, No. 1, pp 99-138.

Campbell, K.W., and Bozorgnia, Y. (2008), "Ground motion model for the geometric mean horizontal component of PGA, PGV, PGD and 5% damped linear elastic response spectra for periods ranging from 0.01 to 10.0 s", *Earthquake Spectra*, Vol. 24, No. 1, pp 139-171.

Chiou, B., and Youngs, R. (2008), "A NGA model for the average horizontal component of peak ground motion and response spectra", *Earthquake Spectra*, Vol. 24, no. 1, pp 173-215.

DMR (1996) Department of Mineral Resources, *Environmental Impact Assessment: Geological Aspect, Kaeng Sua Ten Dam Project, Changwat Phrae*, Main Report No. 3, Ministry of Industry, Thailand.

EGAT (1998) Electricity Generating Authority of Thailand, *Preliminary Seismic Hazard Evaluation of Khao Laem and Srinagarind Dams, Thailand*, Thailand.

Gardner, J. K. and Knopoff, L. (1974), "Is the sequence of earthquakes in southern California, with aftershocks removed, Poissonian?," *Bull. Seism. Soc. Am*., Vol. 64, pp 1363-1367.

Harmsen, S., (2007), *USGS Software for probabilistic Seismic Hazard Analysis (PSHA) Draft Document*, U.S.Geological Survey. (http://earthquake.usgs.gov/research/hazmaps/product_data/2008/software)

Heaton, T.H., Tajima, F. and Mori, A.W. (1986), "Estimating ground motions using recorded accelerograms", *Surveys in Geophysics*, Vol. 8, pp 25-83.

Nutalaya P., Sodsri S. and Arnold E.P. (1985), *SEASEE Series on Seismology, Vol II - Thailand,* Southeast Asia Association of Seismology and Earthquake Engineering and U.S. Geological Survey.

RID (2005) Royal Irrigation Department, *Seismic Hazard Evaluation of The Tha Sae Project, Thailand*, Final Report prepared by URS Corporation.

Scordilis, E.M. (2006), "Empirical global relations converting M_S and m_b to moment magnitude'', *Journal of Seismology*, Vol. 10, pp 225-236.

Sipkin, S.A. (2003), "A correction to body-wave magnitude m_b based on moment magnitude M_W", *Seismological Research Letters,* Vol. 74, No. 6, pp 739-742.

Socquet, A., Vigny, C., Chamot-Rooke, N., Simons, W., Rangin, C., and Ambrosius, B. (2006), "India and Sunda plates motion and deformation along their boundary in Myanmar determined by GPS", *Journal of Geophysical Research*, Vol. 111, 11 p.

Stepp, J. C. (1973), " Analysis of completeness of the earthquake sample in the Puget Sound area, in "Seismic Zoning", edited by S.T. Harding, *NOAA Tech. Report ERL 267-ESL30,* Boulder, Colorado.

Tinti S., Mulargia F. (1985), "Completeness Analysis of a Seismic Catalog", *Annales Geophysicae*, Vol. 3, pp 407-414.

Youngs, R.R., Chiou, S.J., Silva, W.J., and Humphrey, J.R. (1997), "Strong ground motion attenuation relationships for subduction zone earthquakes", *Seismological Research Letters*, Vol. 68, No.1, pp 58-73.

Wells, D.L. and Coppersmith, K.J. (1994), "New empirical relationships among magnitude, rupture length, rupture width, and surface displacements", *Bull. Seism. Soc. Am.,* Vol. 84, pp 974-1002.

Zhao, J. X., Zhang, J., Asano, A., Ohno, Y., Oouchi, T., Takahashi, T., Ogawa, H., Irikura, K., Thio, H., Somerville, P., Fukushima, Y., and Fukushima, Y. (2006), "Attenuation relations of strong ground motion in Japan using site classification based on predominant period", *Bull. Seism. Soc. Am.,* Vol. 96, pp 898-913.

List of Figures

INTERNATIONAL CENTER FOR URBAN SAFETY ENGINEERING
Institute of Industrial Science, The Universiy of Tokyo
4-6-1 Komaba, Meguro-ku,
Tokyo 153-8505, Japan
http://icus.iis.u-tokyo.ac.jp
E-mail: icus@iis.u-tokyo.ac.jp

Tel: (+81-3)5452-6472 ***Fax: (+81-3)5452-6476***